Fragmentation of nuclei by particles and nuclei of intermediate and high energies

Yu. P. Yakovlev

S. O. Makarov Higher Naval Engineering College, Leningrad
Fiz. Elem. Chastits At. Yadra **14**, 1285–1335 (November–December 1983)

The present state of investigations into the fragmentation of target nuclei by particles and nuclei of intermediate and high energies is reviewed.

PACS numbers: 25.40.Ve, 25.70.Np

INTRODUCTION

During the last 5–10 years interest in fragmentation has grown. For this there are many reasons. First, fragmentation data are now widely used to solve many problems in cosmic physics and cosmic chemistry, and this has meant that they must be determined much more accurately and fully. Second, it is in fragmentation reactions that new isotopes of light nuclei have been found[1-4] and searches are made for other unusual nuclear systems,[5-6] including the hypothetical multineutron nuclei. Third, after the work of Thibault-Philippe on the production of heavy fragments (isotopes of sodium from fragmentation of ^{92}Mo and ^{100}Mo by high-energy protons) and the work of the Leningrad groups, who found "isotope effects" for the cross sections and spectra of light slow fragments (isotopes of hydrogen, helium, lithium, beryllium, boron, and carbon[8-10]) and the investigation of Batist *et al.*[11] on isotope effects for ^{17}N heavy fragments, it became clear that new ways had been found to investigate the fragmentation process itself.

The phenomenon acquires particular interest because of the development of new ideas in the physics of hadron–nucleus and nucleus–nucleus interactions (in the present case, these ideas relate to the production of fast fragments). The main directions that have been and are being developped in the physics of fast fragments are the nuclear-fireball model.[12-14] the flucton model,[15,16] and the coalescence model.[17,18] Certain hopes are also placed on the fragmentation phenomenon in connections with the search for hydrodynamic excitation modes of nuclei.[19-21] These ideas, so different in content and in outlook, have stimulated many experimental studies (for example, Refs. 22–38), which have yielded interesting material that has not received its adequate theoretical interpretation.

The development of the experimental possibilities (in particular, the use of beams of relativistic nuclei at the accelerators at Dubna and Berkeley) has led to a rapid growth in the number of publications related to one way or another to the fragmentation problem.

The situation in this branch of physics has changed appreciably during the time that has elapsed since the middle of the seventies. Indeed, by analyzing the available experimental material one can now seek to answer the question of what new insights can, strictly speaking, be gained by studying fragmentation.

The material of the review is divided into three parts. The first concerns the data on light slow fragments and model descriptions of their production; the second, heavy fragments (among which we include nuclei with mass numbers $15 \leqslant A_f \leqslant 50$, provided A_f is appreciably less than the mass number A_0 of the target nucleus). The third group of data concerns fast fragments (light fragments with energies E greater than 10 MeV/nucleon).

We do not consider in detail theoretical studies of fragmentation. There are plenty of reasons for this. In particular, it is not long since the authors of the various theoretical approaches to the physics of fast fragments published review papers: Baldin[39] (see also the review of Stavinskii[26]), Luk'yanov and Titov,[15] Komarov,[41] and Frankfurt and Strikman.[16,40] Therefore, in the corresponding section we shall merely present the physical essence of the models of fast-fragment production and compare the main results with the experiments. Models not included in the reviews of Refs. 15, 16, 26, and 39–42 are here considered in detail, which, of course, does not mean that they appear to us to be more important, even in the case of good agreement with experiment. It is simply that, irrespective of the advantages and shortcomings, they form part of the picture of modern high-energy nuclear physics and to some extent characterize the state of the study of the problem.

With regard to light slow fragments, we restrict the treatment to models associated with pre-equilibrium decay of the nuclei. As yet, these are nothing more than phenomenological and heuristic models, but they do make it possible to avoid a number of difficulties that appear in the development of models of equilibrium decay (see Refs. 42 and 43). In these models, it has been possible to obtain some concerte results that can with value be compared with experiment (see, for example, Refs. 43–46). No attempt has yet been made to derive the model of pre-equilibrium fragmentation, since the development of simpler problems of nuclear kinetics has not yet achieved the present-day level of solution of such problems in statistical physics (see, for example, Ref. 47).

More important at the present time is the actual construction of fragmentation models, their comparison with experiment, systematization of the results, and analysis of the disagreements with the experiments.

It is, however, absolutely clear that fragmentation

 0090-4759/83/060541-22$04.40

is a strongly nonequilibrium process,[43,48,49] related in some way to the development of a nuclear cascade and subsequent relaxation of the nucleus. The nature of the connections and the relationships of the fragmentation characteristics with the properties of the bombarding particles, the target nuclei, and the fragments—these are the problems on which we attempt to cast light in the present review.

1. LIGHT SLOW FRAGMENTS

1.1. Excitation functions and dependence of the cross sections on the mass number A_1 of the bombarding nucleus

The measurements made in recent years of the cross sections for production of fragments following bombardment of nuclei by particles and nuclei at various energies[50-62] have determined more accurately the behavior of the excitation functions. Figures 1 and 2 give examples of these functions for the production of various light slow fragments for various target nuclei. The fragmentation cross sections σ_f increase rapidly in the region $E_p = 2-3$ GeV, after which they tend to a plateau, though for the $p + \mathrm{Al} \rightarrow {}^{7}\mathrm{Be}$ reaction it is not possible to rule out the existence of a maximum of the excitation function for E_p in the range from 2 to 5 GeV.

An interesting feature of the excitation functions is, as can be seen from Fig. 1, the fact that light slow fragments that are isotopes of the same element have approximately the same behavior of the cross sections as E_p increases. It follows from this that one can expect the form of the isotope distributions of the fragments to remain approximately the same with increasing E_p. This is indeed the case (Fig. 3). Moreover, it is found that the shape of the isotope distributions remains the same even on the transition from bombardment of nuclei by protons of various energies to bombardment by fast nuclei. On the other hand, the shape of the isotope distributions is different for different target nuclei A_0 and for different charges Z_f of the fragments. Evidently, ine can write down the factorization relation

$$\sigma_f(A_1 + A_0 \rightarrow A_f) \approx F_1(A_1, A_0)\, F_2(A_0, A_f), \qquad (1)$$

where F_1 depends on only the properties of the target nucleus A_0 and the mass number A_1 (and energy E_1) of

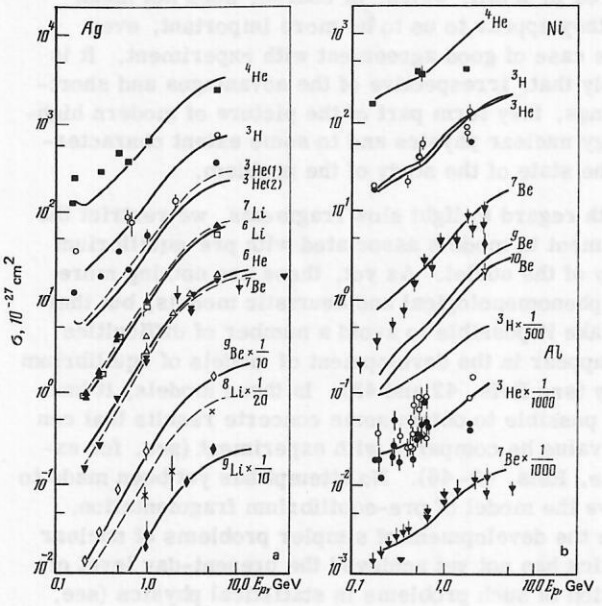

FIG. 1. Excitation functions of the fragmentation reaction on various nuclei. a) ^{3}He: 1) $\langle r^2\rangle^{1/2} = 2.1\times10^{-13}$ cm, 2) $\langle r^2\rangle^{1/2} = 2.5\times10^{-13}$ cm (for ^{4}He*); ^{6}Li (open squares), ^{6}He (open triangles); b) Ni: ^{3}H (open circles), ^{3}He (black circles), ^{9}Be (black diamonds); Al: ^{3}H (open circles), ^{3}He (black circles). The experimental data are taken from Refs. 42, 43, 51, 58, 78, 79, and 81.

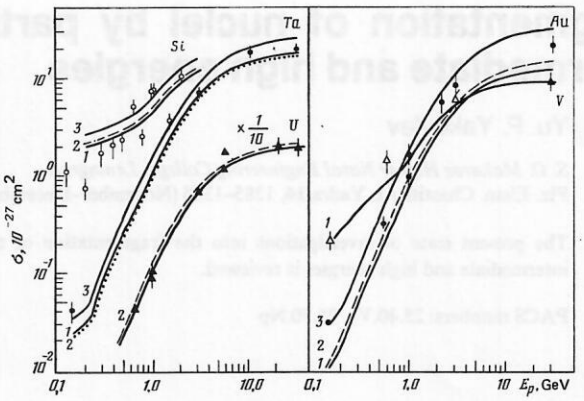

FIG. 2. Excitation functions for ^{7}Be production on light, medium, and heavy nuclei: 1) $g \sim A_0$; 2) $g \sim A_0$, where the masses, except the ^{7}Be mass, are calculated in the liquid-drop model; 3) $g \sim A_0^{2/3}\times 2(\overline{J}_Z + \overline{J}_N + 1)$. The experimental data are taken from Refs. 8, 43, 50–53, 55, 59, and 77–81.

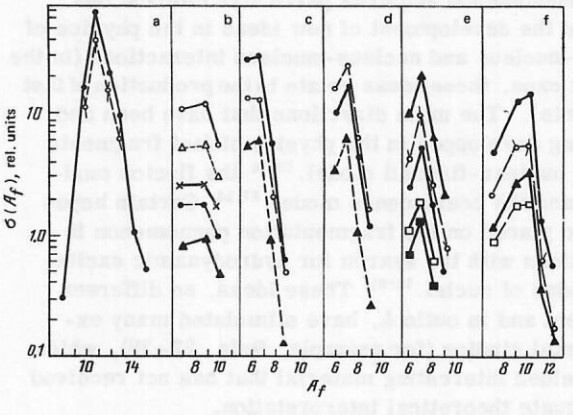

FIG. 3. Isotope distributions of light fragments: a) $p + \mathrm{U} \rightarrow {}^{j}$B: open circles for $E_p = 1.0$ GeV, black circles for $E_p = 5.5$ GeV; b) $p + \mathrm{Ag} \rightarrow {}^{j}$Be: black circles for $E_p = 0.21$ GeV, open circles for $E_p = 0.3$ GeV, black triangles for $E_p = 0.48$ GeV, open triangles for $E_p = 1.0$ GeV, crosses for $E_p = 5.5$ GeV; c) $A_1 + {}^{112}\mathrm{Sn} \rightarrow {}^{j}$Li: black circles for $E_p = 1.0$ GeV, open circles for $E_p = 6.7$ GeV, black triangles for $E_\alpha = 15.3$ GeV; d) $A_1 + {}^{124}\mathrm{Sn} \rightarrow {}^{j}$Li (notation the same as in Fig. 3c); e) $A_1 + \mathrm{U} \rightarrow {}^{j}$Li: open circles for $E_p = 1.0$ GeV, black circles for $E_p = 5.5$ GeV, black triangles for $E_\alpha = 8.4$ GeV, black squares for $E_{^{12}\mathrm{C}} = 25.2$ GeV, open squares for $E_{^{20}\mathrm{N}} = 42.0$ GeV; f) $A_1 + \mathrm{U} \rightarrow {}^{j}$Be (notation the same as in Fig. 1e). The experimental data are taken from Refs. 28, 42, 53, 57, 58, 67, 72, and 73.

the bombarding particle, while F_2 depends effectively on only the properties of the target nucleus and the fragment. The relation (1) recalls the well-known relation of Heckman *et al.*[63] for the fragmentation of relativistic light nuclei on nuclei:

$$\sigma_f(A_1 + A_0 \to A_f) \approx f_1(A_1, A_0) f_2(p + A_0 \to A_f), \quad (2)$$

where f_1 is a function of arguments related to the nuclei A_1 and A_0, and f_2 is the cross section of the $p + A_0 \to A_f$ reaction. This similarity suggests that the relation (1) could be particularized to

$$\sigma_f(A_1 + A_0 \to A_f, \ \Delta A) \approx \sigma_{in} \Delta A F(\Delta A) f(E_1, A_0, A_f), \quad (1')$$

where $\sigma_f(\ldots, \Delta A)$ is the cross section for production of a fragment in a disintegration with ΔA nucleons knocked out of the nucleus, σ_{in} is the total cross section for inelastic interaction of the nucleus A_1 with the nucleus A_0, $F(\Delta A)$ is the distribution (normalized to unity) of the disintegration over ΔA, and $f(E_1, A_0, A_f)$ is a function of its arguments that has the property that with increasing E_1 it hardly changes the isotope distribution of the fragments for given Z_f (for example, the dependence of f on E_1 may be determined by the lowering of the Coulomb varrier when protons are knocked out). It follows from the relation (1′) that for the total fragmentation cross section (summed over ΔA) we must have

$$\sigma_f(A_1 + A_0 \to A_f) \approx \sigma_{in} \langle \Delta A \rangle f(E_1, A_0, A_f). \quad (1'')$$

If we consider the relative yields of fragments induced by the particles A_1, i.e., $Y^{\alpha}_{A_1} = \sigma_f(A_1 + A_0 \to A_f)/\sigma_f(A_1 + A_0 \to \alpha)$, then it can be expected in accordance with (1″) that $Y^{\alpha}_{A_1} \approx f_1(E_1, A_0, A_f)/f(A_1, A_0, \alpha)$, i.e., $Y^{\alpha}_{A_1}(A_f)$ does not depend on A_1. In Fig. 4, this conclusion is confirmed for a number of interesting cases. Thus, for particles A_1 of relatively low energy around 0.1 GeV it is not the case that $Y^{\alpha}_{A_1}$ is independent of A_1 (Fig. 4a). For relativistic particles A_1, the value of $Y^{\alpha}_{A_1}$ is indeed almost independent of A_1. This is also demonstrated in Fig. 4c, in which we give the isotope ratios $y = \sigma_f(A_f, {}^{112}\text{Sn})/\sigma_f(A_f, {}^{124}\text{Sn})$ of the cross sections for bombardment of the maximally stable isotopes of tin by relativistic protons and α particles. It is readily seen that even for the ^{11}Li fragments with their relatively unusual composition the agreement of the $y(p)$ and $y(\alpha)$ values is very good.

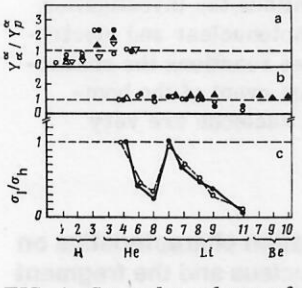

FIG. 4. Some dependences for the relative cross sections $Y^{\alpha}_{A_1} = \sigma_f(A_1 + A_0 \to A_f/\sigma_f(A_1 + A_0 \to \alpha)$ for the production of light slow fragments: a) $E_p = 0.09$ GeV, $E_\alpha = 0.14$ GeV. Target nuclei: black circles for Al, open circles for Ni, black triangles for Zr, inverted open triangles for Bi[60,61]; b) $Y^{\alpha}_{\alpha}/Y^{\alpha}_{p}$ for relativistic values of the energy E_1. Target nuclei: black circles for ^{112}Sn, open circles for ^{124}Sn (E_p = 6.7 GeV, E_α = 15.3 GeV[72,73]), black triangles for U (E_p = 4.9 GeV, E_α = 8.4 GeV[72,74]); c) open circles for $Y^{\alpha}_{p}(^{112}\text{Sn})/Y^{\alpha}_{p}(^{124}\text{Sn})$, black circles for $Y^{\alpha}_{\alpha}(^{112}\text{Sn})/Y^{\alpha}_{\alpha}(^{124}\text{Sn})$, E_p = 6.7 GeV, E_α = 15.3 GeV.[72,73]

TABLE I. Characteristics of disintegration reactions of AgBr nuclei induced by various relativistic nuclei.[67]

A_1	E_1, GeV/nucleon	$\langle n_b \rangle$	$\langle n_g \rangle$	$\sigma_f(A_1 + \text{AgBr} \to {}^{8,9}\text{Li})$	
				calculation	experiment
p	3.0	6.2±0.4	3.4±0.2	8	~8
d	4.0	6.0±0.7	4.5±0.3	15±4	18±4
α	3.5	5.8±0.4	5.9±0.3	21±4	29±6
^{12}C	3.5	6.2±0.4	8.0±0.3	37±8	32±5

A more direct verification of the relation (1″) was made in Ref. 64 on the vasis of an analysis of the data on the production of ^{8,9}Li nuclei by relativistic protons and nuclei on the nuclei of AgBr photographic emulsion. Indeed, assuming that in the region of relativistic energies E_1, where the mean characteristics of the nuclear cascade reach saturation, the function f is also independent of E_1, we can estimate the part played by the first two factors in (1″), making the assumption that $\langle \Delta A \rangle$ is proportional to $\langle n_g \rangle$, the mean number of "gray" prongs resulting from disintegration of the AgBr nuclei:

$$\sigma_f(A_1 + A_0 \to A_f) \approx \sigma_{in}(A_1 + A_0) \langle n_g \rangle_{A_1 + A_0} f'(A_0, A_f). \quad (3)$$

Using the known data[43] on the $p + \text{AgBr} \to {}^{8,9}$Li cross sections, the approximation in Ref. 66 for the $\sigma_{in}(A_1 + A_0)$ cross sections, and the data on $\langle n_g \rangle_{A_1 + \text{AgBr}}$ collected in Ref. 67, we can estimate the cross sections $\sigma_f(A_1 + A_0 \to {}^{8,9}\text{Li})$ for reactions induced by relativistic nuclei (Table I). The agreement with experiment is fairly good. It follows from the same table that when nucleu are bombarded by nuclei no correlation is observed between the mean number of "black" prongs $\langle n_b \rangle$ and the fragmentation cross sections. According to Ref. 66, the mean number $\langle n_b \rangle$ is proportional to the excitation energy of the U nucleus in disintegrations of the AgBr nuclei. Thus, a clear correlation between σ_f and U is not observed. However, in the case of the bombardment of nuclei by protons it follows from the results of cascade calculations[43] that there is the approximate relation $U \sim \Delta A$, i.e., $n_b \sim \Delta A$.

If this is so, then for the $p + \text{AgBr} \to A_f$ reactions, using the relation (1′), we can find that the distribution $F_f(n_b)$ of disintegrations with fragments over the number of "evaporated" particles n_b is given by[67]

$$F_f(n_b) \sim n_b F_0(n_b), \quad (4)$$

where $F_0(n_b)$ is the distribution over n_b of all distintegrations.

In Fig. 5, the relation (4) is compared with the experimental $F_f(n_b)$. In this case too the agreement is reasonable although the experimental distributions F_f are shifted somewhat to the right compared with the calculated ones.

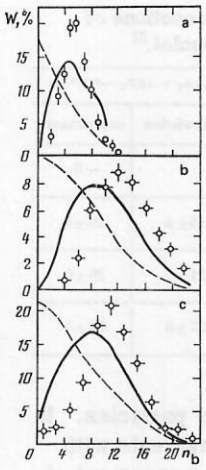

FIG. 5. Experimental (points) and calculated (continuous curves) distributions of disintegrations of AgBr nuclei with respect to the number n_b of black prongs: a) E_p=0.66 GeV; b) E_p=9 GeV; c) E_p=250 GeV. The broken curves are the distribution with respect to n_b of disintegrations without fragments. The figure is taken from Ref. 67.

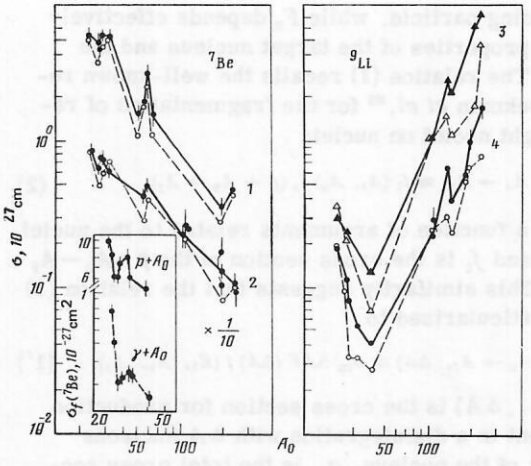

FIG. 6. Cross sections for production of ^{7}Be and ^{9}Li fragments. The black symbols correspond to the experiments, the open symbols to the calculation for $g \sim A_0$: 1) E_p =0.5–0.66 GeV. The sequence of points corresponds to Na, Al, Si, S, V, Fe, ^{58}Ni, ^{64}Ni, Au, U; 2) E_p=1.0 GeV. The sequence of points corresponds to Na, Al, Si, S, Fe, Ni, Ag, Au, U; 3) E_p=2.8 GeV. The sequence of points corresponds to Na, Al, Si, –, Ca, Ag, La, Pr, Pb, U; 4) E_p=1.0 GeV. The sequence of points corresponds to Na, Al, Si, S, Ca, Ag, La, Pr, Ta, Au, U. The inset shows the cross sections for E_p=1.0 GeV and E_γ^{max}=4.5 GeV ($p+A_0$: ^{24,25,26}Mg, Al, S, P, K; $\gamma+A_0$: ^{25,26}Mg, Al, Si, S, Ca). The experimental data are taken from Refs. 8–11, 42, 50, 53, 56, and 58.

The approximate fulfillment of the relations (1′) and (1″) permits a conclusion to be drawn with regard to the possible natue of the production processes of light slow fragments. Evidently, if the fragmentation cross sections were determined by the excitation energy or the degree of disintegration of the nucleus by the cascade [not taken into account solely by the factor $\Delta A F_0(\Delta A)$], the unchanged form of the isotope distributions with changing E_1 and A_1 would be extremely strange (we recall that the fragmentation cross sections for the fragment isotopes differ by tens and hundreds of times for different values of A_1 and E_1!), since this would require very accurate compensation of the variations in the energy of separation of a fragment from the nucleus when the composition is changed, the growth of the excitation energy, etc.

As a working hypothesis, it may be assumed that the process of production of light slow fragments develops over times too short for the state of the nucleons in the nucleus that are not involved in the cascade to change but not so short as to reveal a difference in the development in time of the cascade process for different values of E_1 and A_1, i.e., the process develops over times greater than the cascade development time $t_c \approx 10^{-23}$ sec:

$$t_c < t_f < t_0, \tag{5}$$

where t_0 is the time of rearrangement of the states of the nucleons of the nucleus (for example, in terms of the exciton model of pre-equilibrium states,[43] we can interpret t_0^{-1} as the probability of transitions with a change in the number n of excitons by $\Delta n = 0$). It is possible that the large spread of points in Fig. 4a is due to the fact that the primary particles with energy $E_1 \approx 0.1$ GeV introduce a relatively low excitation energy and "activate" the nucleus so slowly, because of the slow rate of development of the cascade, that there arises a sensitivity to the development of the nuclear activation process, which, naturally, is different for primary protons and α particles.

To conclude this subsection, we give new and very interesting data obtained[68] by bombarding light nuclei with photons of a bremsstrahlung spectrum with E_γ^{max}=4.5 GeV. In Fig. 6a, we give together the cross sections for the production of ^{7}Be following bombardment of the nuclei ^{24,25,26}Mg, ^{27}Al, ^{28}Si, ^{31}P, ^{32}S, ^{39}K by protons with energy 1.0 GeV and ^{25,26}Mg, ^{27}Al, ^{28}Si, ^{31}P, ^{32}S, ^{40}Ca by photons with energy E_γ^{max}=4.5 GeV. The general form of the $\sigma_f(^7\text{Be}, A_0)$ curves in the two cases is similar, but the details are different. It would be very interesting to continue the investigation of fragmentation reactions in photonuclear and electronuclear reactions, since in these reactions the characteristics of the initial interaction event of the bombarding particle with the target nucleons are very different.

1.2. Dependence of fragmentation characteristics on the properties of the target nucleus and the fragment

The accumulated experimental material makes it possible to follow the dependence of the cross sections for the production of light slow fragments on the properties of both the target nucleus and the fragments. Examination of the excitation functions (see Figs. 1 and 2) already gives an indication of how they depend on these properties. It is found that the heavier the target nucleus or the larger Z_f, the more rapid the rate of growth of the cross sections with increasing

E_p. Moreover, the larger Z_0 or Z_f, the longer it is before the cross sections reach a plateau. These are "large-scale" features of the dependence of the cross sections on the properties of the target nucleus and the fragment. The available data, in particular the data relating to the bombardment of target nuclei representing separated isotopes of a number of elements, reveal even more interesting details. For example, there is a different behavior of the A_0 dependence of the cross sections for neutron-rich and neutron-deficient light slow fragments. Figure 6 gives examples of such dependences for ^{7}Be and ^{9}Li fragments for a number of E_p values. The nature of the A_0 dependence of the cross sections for ^{7}Be and ^{9}Li is quite different, but in both cases there is a "fine structure" of the A_0 dependence. For target nuclei with similar A_0, the ^{7}Be yield is greater for isotopes with smaller $N_0 - Z_0$, while for ^{9}Li it is the opposite. It is interesting that this dependence on $N_0 - Z_0$ and $N_f - Z_f$ is even more strongly manifested for the cases when ^{7}Be or ^{9}Li are residual nuclei. It was shown in Refs. 50, 69, and 70 that in this case the dependence of the cross sections on the properties of the target nucleus and the fragment is basically given by "statistical factors," i.e.,

$$\sigma(A_f) \sim \sigma_{\text{in}} \frac{\prod_k (2s_k+1)}{2s_0+1} \exp\left[-\frac{1}{\tau}(Q_{f,k}+B_f)\right], \qquad (6)$$

where s_k are the spins of the products of the cluster breakup of the target nucleus with separation of the cluster A_f, s_0 is the spin of the target nucleus, $Q_{f,k}$ is the energy of separation of the cluster A_f in the given channel, B_f is the Coulomb barrier in the channel, and τ is a "temperature."

Evidently, for the cases when ^{7}Be and ^{9}Li are fragments the "statistical factors" also play an important part. In what follows, on the basis of a model approach to the problem, we shall show that this is the case, although the dependence of the fragmentation cross sections on the properties of the target nucleus and the fragment is not exhausted completely by the dependence on $\langle \Delta A \rangle$, Q_f, B_f, s_f (the fragment spin).

In recent years, investigations have been made of the isotope ratios of the cross sections for production of light slow fragments for fragments with very large values of the isospin T_f, namely, ^{8}He and ^{11}Li.[73] It can be seen from Fig. 7a in which we give the ratios of the cross sections for the production of light slow fragments on the nuclei ^{112}Sn and ^{124}Sn (normalized to the α-particle yields), that for large values of $T_{3,f} = \frac{1}{2}(N_f - Z_f)$ these isotope ratios deviate rather strongly downward from the ordinary exponential dependence at small $T_{3,f}$. It is also interesting that as E_p is increased from 0.66 to 6.7 GeV the slope of the dependence of the isotope ratios on $T_{3,f}$ changes somewhat.

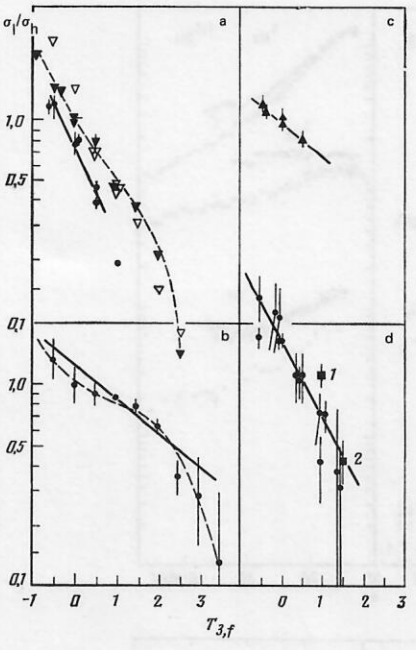

FIG. 7. Isotope effects for fragment production cross sections: a) Light slow fragments, target nuclei ^{112}Sn and ^{124}Sn. The cross sections are normalized to the α-particle yield: inverted black triangles for $E_p = 6.7$ GeV, experiment; open inverted triangles for $E_p = 6.7$ GeV, calculation in the framework of the model of pre-equilibrium fragmentation (see Sec. 1); black circles for $E_p = 0.66$ GeV; b) the reaction $p + ^{10,11}$B $\rightarrow {}^{j}$H, ^{k}He, $E_p = 0.66$ GeV; c) the reaction $p + ^{92,101}$Mo $\rightarrow {}^{j}$Na, $E_p = 25$ GeV; d) target nuclei ^{112,124}Sn, $E_p = 1.0$ GeV: black circles for light slow fragments; 1) ^{24}Na, 2) ^{17}N. The experimental data are taken from Refs. 8–11, 42, 67, and 71. The curves are drawn for clarity.

1.3. Spectra of light slow fragments

Besides the investigation of the dependence of the fragmentation cross sections on the properties of the target nucleus and the fragment, new data have been obtained on the fragment spectra. Of greatest interest are the results of the study of the A_1 dependence of the spectra[72-74] and the dependence of the isotope ratios of the fragmentation cross sections for different sections of the spectrum.[72] It was already noted in the experiments of the Berkeley group[74] that in the case of bombardment of nuclei by relativistic α particles the spectra of the light slow fragments are broader than in the case of bombardment by protons. This result was confirmed in a number of other studies, in particular, in experiments with relativistic ^{20}Ne ions,[28] in which the spectra of the light slow fragments were found to be even broader than in the α-particle experiments.

The broadening of the spectra of the light slow fragments was also studied[72] in the case of bombardment of the extreme tin isotopes ^{112}Sn and ^{124}Sn with relativistic protons and α particles (Fig. 8). A feature of the spectra in these experiments is that the ratios

$$\chi(E) = \frac{\partial^2\sigma_f(A_1 + {}^{112}\text{Sn} \rightarrow A_f)}{\partial E\, \partial\Omega} \Big/ \frac{\partial^2\sigma_f(A_1 + {}^{124}\text{Sn} \rightarrow A_f)}{\partial E\, \partial\Omega}$$

of the differential cross sections are found to be independent of both A_1 and the fragment energy E. With regard to the dependence of χ on E, this conclusion contradicts the tendency noted earlier in Refs 8 and 42 for $\chi(E)$ to tend to 1 with increasing E for $E_p = 0.66$ GeV. For relativistic bombarding particles, the shape of the spectrum evidently becomes insensitive to the A_0 of the target isotope.

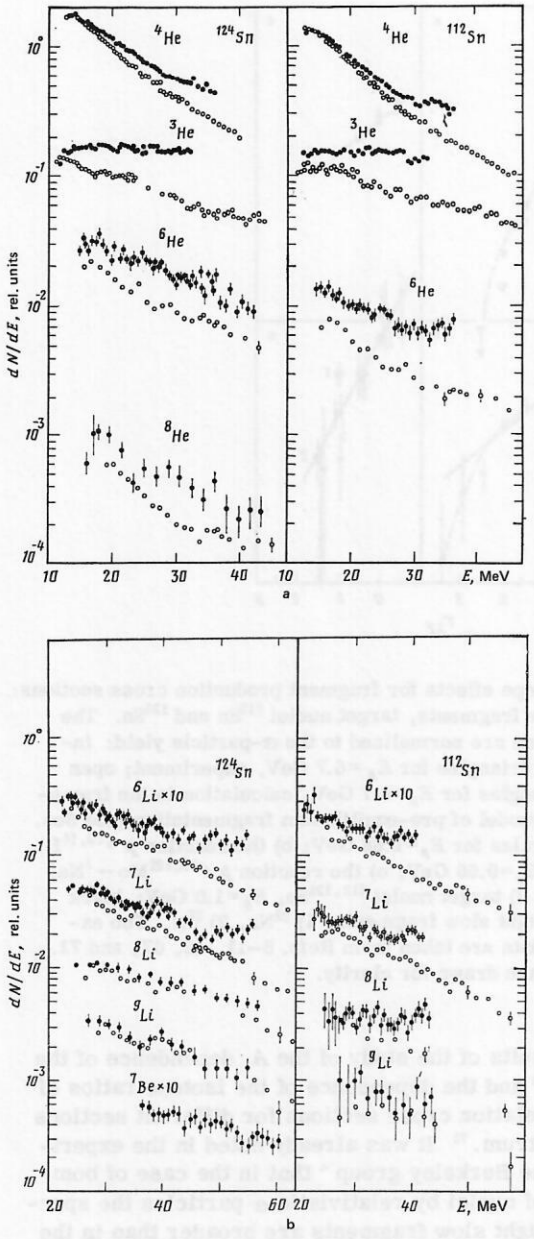

FIG. 8. Energy spectrum of light slow fragments in interactions of protons (open circles) and α particles (black circles) with tin nuclei at E_p=6.7 GeV and E_α=15.3 GeV.[72,73]

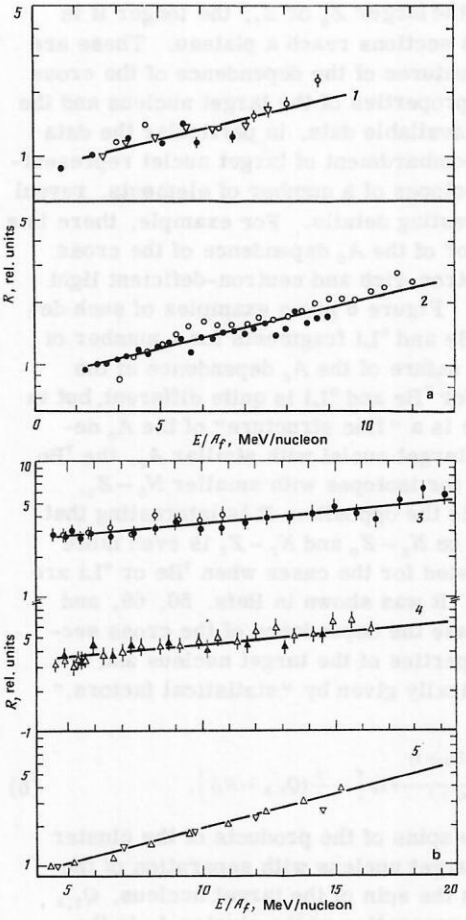

FIG. 9. The ratios $R(E)$ (Refs. 72 and 73): a) for the reaction with ^{124}Sn as A_0 and ^{4}He as A_1, E_α=15.3 GeV, E_p=6.7 GeV; b) the A_1+U→A_f reaction with ^{4}He and ^{20}Ne as A_1; 1) A_f: ^{6}He (black circles), ^{6}Li (open circles), ^{7}Li (open inverted triangles); 2) A_f: ^{4}He (black circles), ^{3}He (open circles); 3) for helium isotopes: black circles for ^{3}He, open circles for ^{4}He, E_p=5.5 GeV, E_α=8.4 GeV; 4) for lithium and beryllium isotopes: open triangles for ^{7}Li, black triangles for ^{7}Be, E_p=5.5 GeV, E_α=8.4 GeV; 5) ^{7}Li and ^{4}He, E_p=5.5 GeV, $E_{^{20}\mathrm{Ne}}$ 042 GeV.

In Ref. 72, an attempt was made to systematize the variations in the shape of the spectra of light slow fragments with increasing A_1. Figure 9 shows the ratios

$$R_{A_1,p}(E)=\frac{\partial^2\sigma_f(A_1+A_0\to A_f,\ E)}{\partial E\,\partial\Omega}\Big/\frac{\partial^2\sigma_f(p+A_0\to A_f,\ E)}{\partial E\,\partial\Omega}. \qquad (7)$$

These ratios can be well approximated by the functions

$$R_{A_1,p}(E)=\exp\left[q_{A_1,p}E/A_f\right], \qquad (8)$$

where $q_{A_1,p}$ depends on A_0 and A_1. For example, for the bombardment of uranium nuclei $q_{\alpha,p}=0.05$ MeV^{-1}, $q_{^{20}Ne,p}=0.13$ MeV^{-1}, while for the ^{122}Sn and ^{124}Sn nuclei $q_{\alpha,p}=0.10$ MeV^{-1}. Thus, the change in the shape of the fragment spectrum with increasing A_1 is characterized by a factor that depends on the square of the fragment velocity (i.e., on E/A_f) but not on the isospoin, A_f, etc. Of course, this is a very provisional conclusion and it would be desirable to study in more detail the dependence of the shape of the spectrum on A_f and $T_{3,f}$. In principle, a deviation of $q_{A_1,p}$ from 0 casts doubt on the significance of the factorization (1′), (1″), since the fragment spectrum is sensitive to both A_0 and A_1. Then together with the frequently used approximation

$$\frac{\partial^2\sigma_f(p+A_0\to A_f,\ E)}{\partial E\,\partial\Omega}\sim(E-B_f)\exp(-E/\tau)$$

we can write

$$\frac{\partial^2\sigma_f(A_1+A_0\to A_f,\ E)}{\partial E\,\partial\Omega}\sim(E-B_f)\exp(-E/\tau'),$$

where

$$\tau'\approx[\tau^{-1}-q_{A_1,\,p}/A_f]^{-1}.$$

For small values of A_f, the difference in the shape of the spectra can be fairly appreciable. The reasons for the change in the shape of the fragment spectra with increasing A_1 are as yet unclear. In Ref. 72, it

TABLE II. Values of the most probable energy $E_{m.p}$ (MeV) and the effective Coulomb barrier B_f (MeV) for bombardment of uranium nuclei by protons with various energies.[81]

Fragment	$E_p = 1.0$ GeV		$E_p = 5.5$ GeV	
	$E_{m.p.}$	B_f	$E_{m.p.}$	B_f
^{4}He	22.1±0.2	16.5	20	12.8
^{6}Li	33.2±0.2	21.9	29	18.2
^{7}Li	33.2±0.2	23.3	31	18.6
^{10}Be	39.7∓0.3	30.3	33	19.7
^{11}B	46.2±0.7	35.1	39,0	23.5

was assumed that this effect is due to "expansion of the exciton gas," this carrying the fragments along with it. Whether this is true or not is at present difficult to say, since the characteristics of disintegrations with fragments initiated by relativistic nuclei have as yet hardly been studied.

One of the properties of the spectra of light slow fragments is the decrease in the most probable energy $E_{m.p}$ of the spectrum with increasing E_p. This effect can be clearly seen for uranium nuclei (Table III). It follows from Table II in particular that the decrease in $E_{m.p}$ is correlated with the decrease in the effective barrier B_f with increasing E_p. This, strictly speaking, is one of the main reasons why with increasing E_p the cross sections for the production of the isotope fragments of one element increase more rapidly than $\langle \Delta A \rangle$ (if $\langle \Delta A \rangle$ is estimated using the data of cascade calculations[43]) and, moreover, equally rapidly for all fragment isotopes, though more rapidly, the larger the Z_0 of the target nucleus [see the relations (1′) and (1″)].

1.4. Model systematization of data on light slow fragments

We consider two systematizations based on the assumption that the process of interaction of high-energy particles and nuclei with nuclei develops in three stages: cascade, evolution to equilibrium, and equilibrium. In all these stages, particles, including fragments, can be emitted. In the considered fragmentation models, it is assumed that the main contribution to the yield of light slow fragments is made by the second, pre-equuilibrium stage.[44-46,75] Use is made

TABLE III. Calculated cross sections of fragment production for bombardment of nuclei with 0.062-GeV protons[44] (the upper number is the pre-equilibrium component, the lower the equilibrium component; the cross sections are given in units of 10^{-27} cm^2).

A_0	Fragment			
	^{2}H	^{3}H	^{3}He	^{4}He
Al	60,29 / 1,32	10,35 / 0,085	8,86 / 0,21	8,69 / 12,8
^{54}Fe	58,5 / 0,82	8,71 / 0,002	15,4 / 0,014	8,54 / 7,50
^{120}Sn	106,2 / 0,44	29,0 / 0,32	4,44 / 0,0003	9,14 / 1,60
Au	103,0 / 0,035	15,4 / 0,011	3,25 / $8\cdot10^{-6}$	4,42 / 0,37

here of the results of cascade calculations realized in accordance with the algorithm given in Ref. 43. This is a fairly typical algorithm, giving satisfactory results not only for the description of the nucleon and meson components of the reaction products but also for the description of the characteristics of the residual nuclei and the fission fragments (see, for example, Refs. 43 and 76).

With regard to other attempts at model description of fragmentation processes (as they relate to light slow fragments) almost exhaustive information about them can be found in the monographs of Refs. 43 and 77, the review of Ref. 42, and Refs. 78–82.

The main idea of the approach used in Refs. 44 and 45 is that in the pre-equilibrum stage the formation of fragments is considered with allowance for not only transitions in which the change in the number of excitons is $\Delta n = 0, \pm 2$ but aso transition of higher multiplicity, i.e., with $\Delta n = -A_f$, which makes it possible to write down the following expression for the probability of emission of fragment A_f:

$$W(A_f, p, h, U, E)\,dE = N(A_f \ldots)\frac{\omega_f}{\omega_i}\lambda_f(E)\,dE, \tag{9}$$

where p is the number of excited nucleons, h is the number of hole excitons ($p+h=n$), U is the excitation energy of the nucleus, E is the fragment energy, $N(A_f)$ is the fragment formation probability, ω_f and ω_i are the density of states of the nucleus after and before emission, and $\lambda_f(E)$ is the "decay rate"[44]:

$$\lambda_f(E) = \frac{(2s_f+1)\,M_f E \sigma_{inv}(E)}{\pi^2\hbar^3 g}, \tag{10}$$

where s_f is the spin of the fragment, M_f is its mass, $\sigma_{inv}(E)$ is the cross section for inverse absorption of the fragment by the nucleus, and g is the density of single-particle states of the target nucleus (for g, a dependence of the following form on the nuclear characteristics is taken[83]: $g \sim A_0 E_F^{-1} \sim A_0 r_0^2$, where E_F is the Fermi energy, and $r_0 = R_0 A_0^{1/3}$, in which R_0 is the radius of the nucleus). It is assumed that $\sigma_{inv}(E) \propto \pi R_0^2 (1 + R_f/R_0)^2$, where R_f is the radius of the fragment nucleus.

In Refs. 44 and 45, the factor $N(A_f)$ is estimated under the assumption that the fragment is formed by the combination of A_f nucleons of the exciton gas. This gives

$$N(A_f) = \gamma(A_f)\,R(A_f, p)\,\omega(A_f, 0, Q_f + E), \tag{11}$$

where the factor $\gamma(A_f)$ is given by the overlap integral of the wave functions of the nucleon component ψ_i of the exciton gas and the cluster function ψ_f (Ref. 44):

$$\gamma(A_f) = \left| \int \psi_1 \ldots \psi_{A_f} \psi_f^* \, d\mathbf{r}_1 \ldots d\mathbf{r}_{A_f} \right|^2 \approx A_f^3 \left(\frac{A_f}{A_0}\right)^{A_f - 1}. \tag{12}$$

The factor $R(A_f, p)$ serves to correct the nucleon composition of the fragment, and ω, which is calculated in the framework of the equidistant model, is the density of states of the A_f nucleons destined to form the fragment (with energy $E + Q_f$, where Q_f is the energy for separation of the fragment from the nucleus). A strong point of the given approach is that the model

does not contain any parameters apart from those usually introduced to describe the nucleon component. The evolution of the system to equilibrium is described in the usual manner in the framework of the exciton model[84] with allowance for transitions with both $\Delta n = +2$ and $\Delta n = -2, 0$. Adding to the pre-equilibrium decay the equilibrium stage of emission of fragments, the authors of Refs. 44 and 45 obtained a very good description of the spectra and cross sections for emission of d, t, and ^{3}He from a number of light, medium, and heavy nuclei at energies E_1 of the bombarding particles up to 0.1 GeV (Fig. 10). The ^{4}He emission cross sections were almost an order of magnitude below the experimental ones. It is interesting that the contribution of the equilibirum component for fragments with $A_f = 2$ and 3 is negligibly small (Table III). If it is assumed that the emission of ^{4}He (in the framework of the considered model) is well described in the equilibrium stage, then for this fragment too the equilibrium stage makes a contribution less than 10%. Thus, the model of Refs. 44 and 45 obviously demonstrated that:

1) the cascade model gives an entirely satisfactorily descripton of the "doorway" states of the fragmenting nucleus;

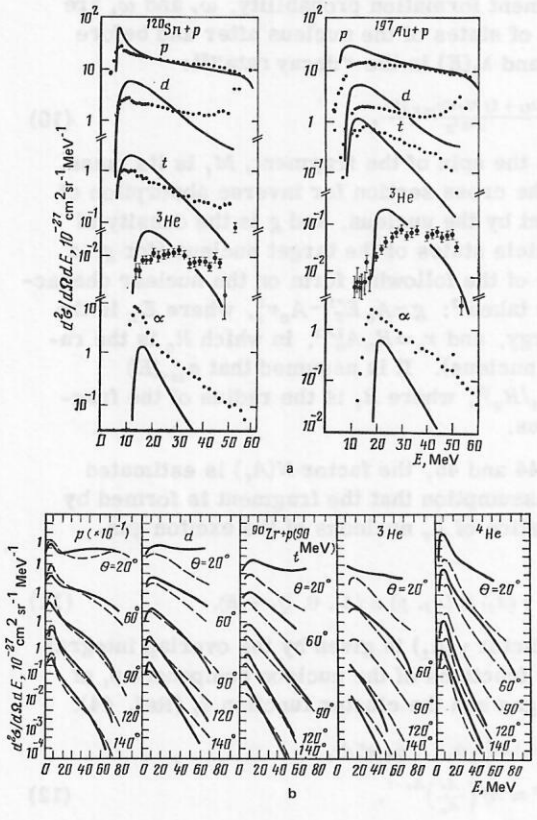

FIG. 10. Comparison with experiment of the double differential cross sections for the production of ^{1}H, ^{2}H, ^{3}H, ^{3}He, ^{4}He calculated in the model of pre-equilibrium fragmentation[44,45]: a) $p + {}^{120}\mathrm{Sn} \to A_f$, $p + {}^{197}\mathrm{Au} \to A_f$, $E_p = 0.062$ GeV; b) $p + {}^{90}\mathrm{Zr} \to A_f$, $E_p = 0.09$ GeV. The points and broken curves represent the experiments, the continuous curves the calculations. The experimental data are taken from Refs. 44, 60, and 61.

2) the contribution of the equilibrium component to the fragmentation cross section is small. This second conclusion corresponds to well-known experimental facts (see, for example, Refs. 42, 48, 49, 57, and 58).

The fact that in the model of Refs. 44 and 45 it was not possible to describe well the data on $A_f = 4$ cannot be regarded as a serious reason for criticizing it, since since, first, one can hardly require from such an extremely simplified model perfect agreement with experiment and, second, the main value of Refs. 44 and 45 is that in them, on the basis of realistic doorway states, evolution with the formation of fragments is described. In Refs. 46, 67, 75, and 85, the model of pre-equilibrium fragmentation is formulated as a development of the evaporation model. The cross section for the fomation of fragments A_f in the k-th excited state is described by the expression

$$\frac{d\sigma_k(A_f, E, \tau_0)}{dE} = \sigma_{\text{in}} F(\Delta A, \tau_0) P(A_f, E, \tau_0), \tag{13}$$

where $F(\Delta A, \tau_0)$ is the distribution of the interactions with respect to the number ΔA of nucleons knocked out and the "temperature" τ_0 (the canonical ensemble is used), and P is the probability of emission of a fragment with energy E:

$$P(A_f, E, \tau_0) = \frac{m_f E' (2s_k + 1)}{\pi^2 \hbar^3 v_{\text{rel}}} |M_f|^2 \omega_f, \tag{14'}$$

where m_f is the mass of the fragment E' and v_{rel} are its energy and velocity of the relative motion, s_k is the spin of the k-th state of the fragment (energy U_k, isospin $T_{f,k}$), and ω_f is the density of the final states of the residual nucleus. Into the ordinary expression $|M_f|^2 = v_{\text{rel}} \sigma_{\text{inv}}(E')/\omega_I$ one introduces the relative probability of transitions to fragmentation states:

$$D_f = P_f(\tau_0, A_f) f(\Delta A, n) \lambda_+^{-1}, \tag{14''}$$

where P_f is the probability of fluctuations leading to rearrangement of the exciton part of the nuclear nucleons with the formation of fragments (of the type of a heterophase transition of the second kind[85]), λ_+ is the probability per unit time of "ordinary" transitions in which the number n of "excitons" changes by $\Delta n = +2$, and f is the efficiency of the "excitons" of various types in the formation of fragments. The competition of nucleon emission is ignored, which for high excitation energies and, especially, small A_0 and A_f must lead to an appreciable overestimation of the cross sections. It is assumed that $P_f \approx \exp(\Delta S_f)$, where ΔS_f is the change in the entropy on the formation of one fragment ($\Delta S_f = -\delta_f/\tau_n$, where $\tau_n^{-1} = \partial S(n, U)/\partial U$ is the "effective temperature" of the n-exciton state of the nucleus; for an equidistant spectrum it is equal to U/n). For δ_f, the following dependence on the properties of the target nucleus and the fragment is assumed:

$$\delta_f = \delta_f^{\text{is}} + \delta_f^{\text{iv}}, \tag{15}$$

where σ_f^j are given by simple functionals:

$$\delta_f^j = \int d^3r d^3r' \rho_f^j(\mathbf{r}) E^j(\mathbf{r} - \mathbf{r}') \rho_1^j(\mathbf{r}'); \tag{16}$$

$$\rho_1^j(\mathbf{r}) = \rho_0^j(\mathbf{r}) - \rho_f^j(\mathbf{r}); \tag{17}$$

$\rho_f^{\text{is}}(\mathbf{r}) = \rho_f(\mathbf{r})$, $\rho_0^{\text{is}}(\mathbf{r}) = \rho_0$ are the matter densities of the

fragment and the target nucleus (in the liquid-drop model, $\rho_0 = 0.17 \times 10^{39}$ cm^{-3} (Ref. 90));

$$\rho_f^{iv}(\mathbf{r}) = \frac{\hat{T}_f}{A_f}\rho_f(\mathbf{r}),\ \rho_0^{iv}(\mathbf{r}) = \frac{\hat{T}_0}{A_0}\rho_0$$

are the isospin densities with neglect of the differences between the proton and neutron distributions.

For E^j the following expression is proposed:

$$E^j(\mathbf{x}) = \varepsilon^j \delta(\mathbf{x})/\rho_0. \tag{18}$$

The coefficients ε^j are taken equal to the parameters of the mass formula in the liquid-drop model with the above value[90] of ρ_0:

$$\left.\begin{aligned}\varepsilon^{is} &= 15{,}68\,(1-1{,}184\,A_0^{-1/3}),\ \text{MeV};\\ \varepsilon^{iv} &= -112{,}4\,(1-1{,}184\,A_0^{-1/3}),\ \text{MeV}\end{aligned}\right\}. \tag{19}$$

For δ_f^j, this gives approximately

$$\left.\begin{aligned}\delta_f^{is} &\approx 15{,}68\,(1-\langle\rho_f\rangle/\rho_0)\,(1-1{,}184\,A_0^{-1/3})\,A_f,\ \text{MeV};\\ \delta_f^{iv} &\approx -\frac{112{,}4}{A_0}\left(\hat{T}_0\hat{T}_{f,k} - \frac{\langle\rho_f\rangle}{\rho_0}\frac{T_{f,k}(T_{f,k}+1)\,A_0}{A_f}\right)(1-1{,}184\,A_0^{-1/3}),\ \text{MeV}.\end{aligned}\right\} \tag{20}$$

Here, $\langle\rho_f\rangle = 1/A_f \int d^3\mathbf{r}\rho^2(\mathbf{r})$, and $T_{f,k}$ is the isospin of the fragment in the k-th excited state (energy U_k, spin s_k).

In addition, in the model it is assumed that: 1) the nucleating centers of the fluctuations are basically fairly long-lived[86-89] defects of the density of the nucleus formed during the cascade (their number is ΔA), which gives $f(\Delta A, n) \approx \Delta A/\bar{n}$, where $\bar{n}$ is the mean number of "excitons" in the given stage of relaxation to equilibrium; 2) λ_+ depends on τ_n and on the density g of the single-particle states in the same way as the decay probability of quasiparticles in a Fermi liquid in the lowest order: $\lambda_+ = a_t^{-1}\tau_n^2 g$. For g, the expression obtained for a degenerate Fermi system[83] is assumed, $g = a_A r_0^2 A_0$, MeV^{-1} (for r_0 measured in 10^{-13} cm, $a_A = 0.0195$). A more realistic expression taking into account the lifting of the degeneracy by the residual interactions and a number of other effects has a complicated structure.[83] In the simplest case, one can write $g = a_j r_0^2 A_0^{2/3} 2[\bar{J}_Z + \bar{J}_N + 1]$, where $2\bar{J}_Z + 1$ and $2\bar{J}_N + 1$ are the averaged multipolarities of the proton and neutron states near the Fermi limit. For some nuclei, in particular, for Pb and those near it, the corrections to $g \sim A_0$ are large.

For semiquantitative analysis it is assumed that $F(\Delta A, \tau_0) \approx F_1(\Delta A)F_2(\tau_0)$. The distributions over ΔA and τ_0 are taken from the data of cascade calculations,[43] and from them estimates are made of the mean quantities: $\langle\Delta A^2\rangle$, the mean excitation energy $\langle U\rangle$ of the fragmenting nuclei, etc. It is assumed that at the end of the cascade and in the relaxation stage the spread of the values of τ_0 and τ_n is described in the same way:

$$F_2(\tau) \approx \frac{1}{\sqrt{2\pi}\,\sigma}\exp\left(-\frac{(\tau-\bar{\tau})^2}{2\sigma^2}\right), \tag{21}$$

where $\bar{\tau}$ is the "mean temperature" in the given stage, and σ^2 is the mean square of its "fluctuation." For an approximate estimate of σ^2, the relation $\sigma^2/(\bar{\tau})^2 \approx 1/(2\bar{n})$ is used, which takes into account the fact that the number of "excitons" changes by +2. In concrete calculations, Eq. (21) was replaced by a step distribution with step 0.5σ and step height ensuring the same area as the section of the Gaussian curve at the given step. To the left of $\bar{\tau}$, three steps were taken; to the right, four. Bearing in mind that δ_f for the fragments is of the order of tens or hundreds of mega-electron-volts, it was assumed that $1/(2\bar{n})^{1/2} \approx 1/(2\bar{n}_0)^{1/2} \approx \sqrt{\tau_0/\langle 2U\rangle_f}$, where $\bar{\tau}_0$ is the mean temperature of the postcascade nucleus. The value of $\langle U\rangle_f$ was estimated under the assumption that $\langle U\rangle$ is approximately proportional to $\langle\Delta A\rangle$.[43] The mean number of nucleons knocked out in the cascade in disintegrations with fragments for $f(\Delta A, n) \sim \Delta A$ can be estimated approximately as $\sum_{\Delta A}\Delta A^2 F_1(\Delta A)/\sum_{\Delta A}\times\Delta A F_1(\Delta A)$, which in accordance with the data of Ref. 43 on $F_1(\Delta A)$ for ^{27}Al, ^{100}Ru, ^{238}U with $E_p < 5$ GeV is approximately $1.5\langle\Delta A\rangle$. The experiment[43] for the mean number $\langle n_g\rangle$ of cascade nucleons and the mean number $\langle n_b\rangle$ of "evaporated" particles gives $\langle n_g\rangle_f/\langle n_g\rangle \simeq 1.8$–$1.5$, $\langle n_b\rangle_f/\langle n_b\rangle \simeq 1.8$–$1.5$. We assume that $\langle U\rangle_f \approx 1.5\langle U\rangle$. After the substitution $\omega_f/\omega_i \approx \exp[-(Q_f + u_k + E')/\tau_n]$, the replacement of summation over n from n_0 ("initial number of excitons") to n_{eq} by integration over $\beta = n/U$ (Ref. 46), $\sum_{\Delta n=+2}^{n\,eq}\cdots \to U/2\int_{\beta_0}^{\infty} d\beta\ldots$, convolution with the chosen distribution of excursions of τ, and summation over ΔA, we have (in units of 10^{-27} cm^2/MeV)

$$\frac{d\sigma_k(A_f, E)}{dE} \approx b\,\frac{m_N\sigma_{in}A_f(2s_k+1)\langle\Delta A\rangle\,\sigma_{inv}(E')}{2\pi^2\hbar^3\lambda_+}\,\Sigma_{fr}, \tag{22}$$

if σ_{in} in 10^{-27} cm^2 is the fragment energy, MeV; b is an adjustable parameter that must be near unity;

$$\Sigma_{fr} = \frac{1}{W^2}\sum_{j=-3}^{j=+4} P(j)\,[1+0{,}5\gamma(j)\,j]\exp[-\beta(j)\,W]; \tag{23'}$$

$W = Q_f + u_k + \delta_f + E'$, $\beta_0 = 1/\tau_0$, $\gamma(j) = \beta(j)\sigma$, $\beta(j) = \beta_0(1 + 0.5j\gamma)$, $\gamma = \beta_0\sigma$; β_0 is a parameter that must be chosen; and $P(j)$ for j from -3 to $+4$ is equal to -0.1837, -0.1163, -0.0829, 0.0, 0.0829, 0.1163, 0.0956, 0.0881. For the barrier height (MeV) the following estimate was obtained (under the assumption that the number of knocked-out protons is $\Delta Z_0 = Z_0\Delta A/A_0$):

$$B_f \approx \frac{Z_f(Z_0 - Z_f)}{R_0 + R_f}\left[1 - \frac{Z_0\langle\Delta A_0\rangle}{(Z_0 - Z_f)A_0}\right]. \tag{23''}$$

The total cross section for production of a fragment in state k is determined by integrating (22) over E. The energy is $E' = EA_t/\mu_t$, where $\mu_f = A_t \times(A_0 - \langle\Delta A\rangle_f) - A_t/(A_0 - \langle\Delta A\rangle_f)$. In the determination of the cross section, allowance is made for the formation of the fragment A_t following decay of a heavier A_t' in states k' which decay through the channel $A_t' \to A_t + X$. It was assumed that the kinetic energy of fragment A_t' is A_t'/A_t times greater than the energy E of fragment A_t. The decay energy of the fragment A_t' was not taken into account. Using the data of Toneev[87] on the mean values of ΔA, U, and the number of cascade collisions in the ^{70}Ga nucleus, one can estimate τ_0.[42,46] This estimate gives $\tau_0 \approx 10$–11 MeV. The parameters $\tau_0(A_0, E_p)$ and b were chosen using the data on the cross sections for the production of ^{7}Be on the nuclei of Al, Ag, U with allowance for this estimate of τ_0 and using the data of Ref. 43 on $\langle\Delta A\rangle$ and $\langle U\rangle$, which gave

$$\tau_0^{-1} \equiv \beta_0 = 0.1\left[1+0.06\left(\frac{A_0-23}{A_0}\right)^2\frac{1}{E_p}\right](1+\sqrt{5.8/\langle U\rangle}). \quad (24')$$

For $\langle \Delta A\rangle$ and $\langle U\rangle$, the following approximations were proposed:

$$\langle \Delta A\rangle = 4\exp\left[\frac{R_0}{r_0^3}\left(0.45-\frac{0.3}{E_p}+\frac{0.03}{E_p^2}\right)\right]$$
$$\times\left[7{,}5\exp\left(-E_p/0.185\right)+\frac{E_p}{E_p+0.5}+0.15\right]\exp\left[-6{,}237/(A_0E_p)\right]; \quad (24'')$$

$$\langle U\rangle = 31\,\langle \Delta A\rangle\left[1+\frac{0{,}3}{(E_p-2)^2+1}\right]^{-1}$$
$$\times\exp\left[-\frac{20.9}{E_pA_0}+\frac{20.3}{E_p\,(20\,E_p+1)\left(1+\frac{A_0}{22.65}\right)^3}\right]. \quad (24''')$$

In Eqs. (24′)–(24‴), τ_0 and U are given in MeV, and E_p in GeV. They give saturaion at large E_p (imitating the "trawling effect"[43]). It was assumed that the fragmentation proceeds rapidly until the nucleus has had time to readjust. This makes it possible to assume that Q_f is close to the energy for separation of the fragment from the target nucleus. The masses of the nuclei are taken from Ref. 90, and the data for calculating $\langle \rho_f\rangle$, R_f, and R_0 from Ref. 91. For $A_f=3$, the values of R_f and $\langle \rho_f\rangle$ were taken to be the same as for ^{3}He. For ^{9}Be there are data on the distribution of not only the charge density but also the matter density. They were used for $A_f=9$. It was assumed that for a given isobar all the R_f and $\langle \rho_f\rangle$ are the same and do not depend on u_k, but for ^{4}He*–^{3}He, ^{3}H the theoretical estimates of the radius of Ref. 99 were used, i.e., $\langle r^2\rangle^{1/2} = 2.5\times10^{-13}$ cm. For $A_f=5$ and $A_f=8$ there are no data on $\rho_f(r)$ and for them values intermediate between $A_f=4.6$ and $A_f=7.9$, respectively, were taken. The probabilities in the channels ^{4}He* → ^{3}He, ^{3}H were taken to be 0.5. The value of $\varphi = a_f/a_A$ [or (a_f/a_J)] was estimated using the data of Ref. 84 for the system with $A_0=64$, $n=3$, $U=24$ MeV, for which $\lambda_+ \approx 0.5\times10^{22}$ sec^{-1}. This gives $\varphi \approx 1.18\times10^{-18}$ sec. (For $\tau=10$ MeV and $A_0\approx100$, the relaxation time is $t_n\approx10^{-22}$ sec.)

Assuming $\sigma_{inv}=\pi(1-B_f/E')(R_0+R_f)^2$ (in units of 10^{-26} cm^2) and collecting together the numerical coefficients of the expression (22), choosing b for $g=0.0195r_0^2/A_0$, MeV^{-1} (r_0 in units of 10^{-13} cm), we obtain

$$\frac{d\sigma_k(A_f,\,E)}{dE} = 17{,}45\,\sigma_{in}\,\langle \Delta A\rangle\,(2s_k+1)\,A_0^{-1/3}\,(E'-B_f)\,A_f\,\Sigma_{tr}$$

(in the units 10^{-27} cm^2/MeV, if $\sigma_{in}=\pi R_0^2$ is given in the units 10^{-27} cm^2, and W, E, and B_f are given in MeV). The factor 17.45 is approximately 2.5 times greater than from the expression (22) (for $b=1$). Note that the

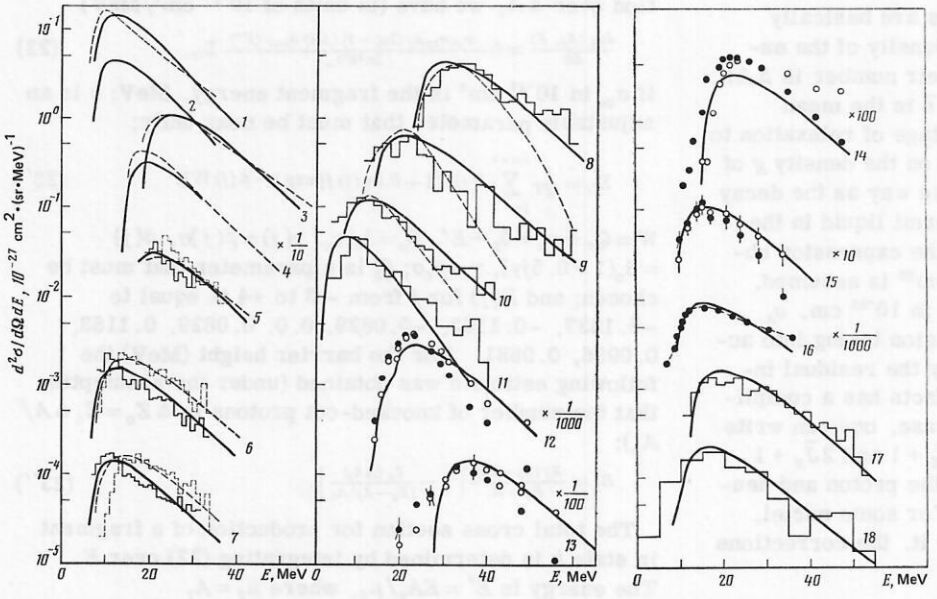

FIG. 11. Comparison with experiment of the calculated spectra of light slow fragments: 1) p (0.156 GeV) + Ag → ^{3}H: the broken curve shows the experiment ($\theta=45°$), the continuous curve the calculation (the normalization is arbitrary); 2) calculation ($\theta=90°$) for p (0.156 GeV) + Ag → ^{3}H; 3) p (0.3 GeV) + Ag → ^{7}Be: the broken curve shows the experiment ($\theta=90°$), the continuous curve the calculation; 4) p (0.21 GeV) + Ag → ^{6}Li: the broken curve shows the experiment ($\theta=90°$), the continuous curve the calculation; 5) p (0.66 GeV) + ^{124}Sn → ^{6,7}Li: the broken curve is for ^{7}Li, the continuous curve for ^{6}Li; the histograms show the experiment ($\theta=90°$), the curves the calculation (the normalization is arbitrary); 6) p (0.66 GeV) + ^{64}Ni → ^{6,7}Li. The notation is the same as for 5); 7) p (0.66 GeV) + ^{58}Ni → ^{6,7}Li. The notation is the same as for 5); 8) p (0.66 GeV) + Th → ^{8,9}Li: the histogram shows the experiment ($\theta=90°$), the broken curve is the calculation in the framework of the cascade–evaporation model of Ref. 49, and the continuous curve is a calculation; 9) p (0.66 GeV) + Ag → ^{8,9}Li. The notation is the same as for 8); 10) p (0.66 GeV) + V → ^{8,9}Li. The notation is the same as for 8); 11) p (0.66 GeV) + Al → ^{8,9}Li. The notation is the same as for 8); for 8)–11) the normalization is arbitrary; 12) p (1.0 GeV) + U → ^{4}He: the continuous curve shows the calculation, the open circles correspond to $\theta=90°$, the black circles to 120°; 13) p (1.0 GeV) + U → ^{9}Be: the notation is the same as for 12); 14) p (1.0 GeV) + U → ^{6}He: the notation is the same as for 12); 15) p (1.0 GeV) + Ag → ^{6}He: the notation is the same as for 12); 16) p (5.5 GeV) + U → ^{2}He: $\theta=90°$, the continuous curve shows the calculation; 17) p (2.2 GeV) + Ag → ^{8,9}Li: the continuous curve shows the calculation (arbitrary normalization); 18) p (250 GeV) + AgBr → ^{8,9}Li: the continuous curve shows the calculation (arbitrary normalization). The calculated cross sections are obtained under the assumption that $d\sigma_f/d\Omega \approx a+b\cos\theta$. The experimental data are taken from Refs. 43, 48, 49, 57, 58, 80, 81, 95, 97, and 98.

variants of the model in which effective roles are played either by all the excitons, or only the nucleon excitons, or all hole excitons would give a smaller deviation of the normalizing factor from the theoretical value but would change little otherwise. However, the inaccuracies in the estimate of φ and the other inaccuracies of the model do not permit us to conclude which variant of the model is best, and we restrict ourselves to the $f \approx \Delta A/\overline{n}$ considered here.

In Figs. 1, 2, 6, 7, and 11 and in Tables IV and V we give examples of comparison of the calculation with the experiments for $g \sim A_0$. The agreement with the experiments is good, despite the very large range of the cross sections (from about 10^{-29} to about 10^{-24} cm^2). As expected, because of the neglect of nucleon emission and a number of other simplifications, the agreement with the experiments for large E_p and small A_0 and A_t is less good, while for nuclei with $A_0 \approx 200$ the calculated cross sections are significantly smaller than the experimental ones. This can be seen particularly well in Fig. 12, which shows the data, averaged over A_t, on the ratios of the experimental and model cross sections, σ_e/σ_m, and the ratio of $g \sim A_0^{2/3} 2(\overline{J}_N + \overline{J}_Z + 1)$ and $g \sim A_0$. It can be seen that there is a correlation between the ratios of the cross sections and the densities of the levels. The deviation of σ_e/σ_m from 1 is less if one assumes $g \sim A_0^{2/3} 2(\overline{J}_N + \overline{J}_Z + 1)$. There is a similar correlation with σ_e/σ_m for the difference between the experimental values of the masses of the target nuclei and the values determined using the liquid-drop model (the quantities Q_s). Thus, the variant with $g \sim A_0$ and with the shell effects for the masses of the nuclei "switched off" (except for the fragment mass!) can give a reasonable description of the experiments (see

TABLE IV. Cross sections for the production of fragments. Comparison of the predictions of the model of pre-equilibrium fragmentation with experiment. The experimental data are taken from Refs. 9, 42, 55, and 79–81, $g \sim A_0$, Q_f are exact.

A_f	A_0	E_p, GeV	σ_f, 10^{-27} cm^2	
			calculation	experiment
^{2}H	Al	0,19	177	88
		0,60	255	169
	^{58}Ni	0,66 *	196	122±4
	^{64}Ni	0,66 *	160	107±3
	Ag	0,156	122	124±16
^{3}H	Si	0,6	25	36±4
	V	0,6	54	52±8
	^{58}Ni	0,66 *	36	58.3±2,0
	^{64}Ni	0,66 *	52	88.7±3,0
^{3}He	Si	0,6	30,0	42±5
	Ag	0,6	16	21
	Au	0,156	5,1	6,6
^{4}He	^{58}Ni	0,66 *	345	353±4
	^{64}Ni	0,66 *	293	302±4
	Au	1,0	513	1130±140
	U	1,0	722	1070±130
		5,5	5020	4400
^{8}He	U	5,5	2,3	4,2
^{6}Li	U	1,0	6,2	9,8±1,6
		5,5	63,5	73
^{7}Li	U	1,0	13	22,8±3,6
		5,5	124	164
^{8}Li	U	5,5	41	49
^{11}Li	U	5,5	0,19	0,2
^{8}B	U	5,5	0,2	0,3
^{10}B	Ni	3,0	4,6	5,6±1,2
	U	1,0	1,9	1,3±0,2
		5,5	15	16
^{17}B	U	4,8	0,015	0,005
^{13}N	U	0,94	0,053	0,024

*The cross section is obtained by multiplying $d\sigma/d\Omega(\theta = 90°)$ by 4π.

TABLE V. Experimental and calculated cross sections for ^{7}Be production[43,50,53] and their ratios for different E_p. Allowance has been made for the inaccuracy in the approximation of $\langle \Delta A \rangle$. To the right of the chemical symbol of the target nucleus the number of neutrons (superscript) and the number of protons (subscript) are given.

A_0	σ, 10^{-27} cm^2				$\sigma_{exp}/\sigma_{cal}$	
	experiment		calculation			
	0,66 GeV	1,0 GeV	0,66 GeV	1,0 GeV	0,66 GeV	1,0 GeV
^{23}Na$^{12}_{11}$	5,2±0,6	7,0±0,8	4,2	6,6	1,24±0,14	1,06±0,12
^{27}Al$^{14}_{13}$	4,8±0,5	6,2±0,6	3,1	4,7	1,5±0,17	1,31±0,13
^{28}Si$^{14}_{14}$	5,8±0,6	7,5±0,8	3,8	5,7	1,5±0,16	1,30±0,14
^{32}S$^{16}_{16}$	5,1±0,6	6,1±0,7	4,6	6,9	1,11±0,13	0,88±0,10
^{58}Ni$^{30}_{28}$	2,89±0,3 *	4,9±0,6 *	2,3	4,04	1,26±0,13	1,21±0,15
^{61}Ni$^{36}_{28}$	1,31±0,13	—	0,83	—	1,58±0,16	—
^{108}Ag$^{61}_{47}$	0,801 **	2,6±0,7 2,2±0,4	0,64	2,34	1,25	1,03±0,2
^{181}Ta$^{108}_{73}$	—	7,2±0,7 ***	—	6,8 ***	—	1,06± ±0,11 ***
^{197}Au$^{118}_{79}$	0,35± ±0,05 ****	1,3±0,2	0.24 ****	0,90	1,45± ±0,20 ****	1,44±0,22
^{208}Pb$^{126}_{82}$	—	6,2±0,6 ***	—	3,2 ***	—	1,94± ±0,20 ***
^{238}U$^{146}_{92}$	0,45±0,06	0,92±0,21 1,12±0,10	0,48	1,04	0,94±0,13	0,98±0,12

*The cross section is obtained by multiplying $d\sigma$ $(\theta = 90°)/d\Omega$ by 4π.
**E_p = 0.48 GeV.
***E_p = 3.0 GeV.
****E_p = 0.55 GeV.

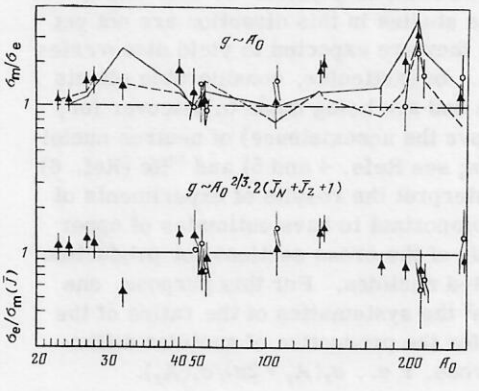

FIG. 12. Ratios of experimental, σ_e, and model, σ_m, cross sections for production of light slow fragments. The black symbols correspond to $A_f \geq 6$, the open symbols to $A_f = 3$ and 4; the continuous line shows the ratio $2(\overline{J}_Z + \overline{J}_N + 1)/A_0^{1/3}$ (normalized to 1 for Ag); the broken line shows $\exp(Q_s/10)$, where Q_s is the difference between the exact mass of the nucleus A_0 and the liquid-drop value (in MeV).[90] The sequence of points corresponds to Na, Mg, Al, Si, S, Ca, V, Fe, Ni, Ag, La, Pr, Ta, Au, Pb, Bi, U. The experimental data are taken from Refs. 42, 50–52, 56, and 58.

Fig. 2). Unfortunately, the available data are inadequate for choosing the variant with "switched-off" shell effects or the variant of the fast process, in which the shells manifest themselves in the values of both Q_f and g.

We shall show below that to describe the characteristics of the $p + {}^{112,124}\mathrm{Sn} \to {}^{17}\mathrm{N}$ reaction the variant with the shells "switched off" is better suited. But for a heavy fragment the formation time t_f may be sufficiently long for such "switching off." In any case, the fact that the shape of the isotope distributions of the light slow fragments remains the same as E_1 and A_1 are varied (see Fig. 3) can be regarded as important evidence in support of a rapid (compared with the time of relaxation to equilibrium) rate of formation of these fragments. Evidently, for the light slow fragments the formation time is in order of magnitude near λ_+^{-1}, i.e., of order 10^{-22} sec.

The considered "models" of fragmentation in no way pretend to a high accuracy or great degree of theoretical cogency. These are models suitable for estimating the possible connections between the characteristics of the target nucleus, the fragment, and the incident particle on the one hand, and, on the other, the fragmentation characteristics. The obtained relations make it possible to systematize a large body of information. In addition, they unite in one approach data on light slow fragments with data on the meson and nucleon components of the disintegration products. However, the true physical significance of these relations remains largely unclear.

1.5. Some questions related to the search for isotopes of light nuclei with unusual nucleon composition

The use of fragmentation reactions to discover and investigate unusual isotopes of light nuclei already gave important results long ago.[1-7] Without going into the details of the reasons why this problem is of great interest for modern nuclear physics, we note that at the present time the studies in this direction are not yet completed, and they are expected to yield discoveries of new nuclides. In particular, considerable efforts have been made and are being made to discover (or, conversely, prove the nonexistence) of neutron nuclei (for example, ${}^{8}n$; see Refs. 4 and 5) and ${}^{10}\mathrm{He}$ (Ref. 6) and ${}^{13}\mathrm{Li}$. To interpret the results of experiments of this kind, it is important to have estimates of upper and lower bounds of the cross sections for production of the investigated nuclides. For this purpose, one sometimes uses[6] the systematics of the ratios of the cross sections for the production of nuclides differing by two neutrons, i.e., $\sigma_f(A_f + 2n)/\sigma_f(A_f)$.

Thus, it was shown in Ref. 6 by this method that the nuclides ${}^{8}n$ and ${}^{10}\mathrm{He}$ do not exist if one proceeds from the upper bounds of the experimental cross sections, while it was concluded that ${}^{13}\mathrm{Li}_3$ may exist. Bearing in mind that the model of pre-equilibrium fragmentation gives a reasonable description of the production characteristics of light slow fragments, we can estimate the extent to which the empirical systematics of the ratios $\sigma_f(A_f + 2n)/\sigma_f(A_f)$ is reproduced by the calculation, and, thus, whether one can believe the extrapolations of these ratios.

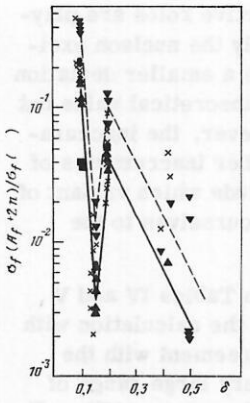

FIG. 13. Comparison of ratios $\sigma_f(A_f + 2n)/\sigma_f(A_f)$ of experimental and calculated cross sections. Calculation for ${}^{64}\mathrm{Ni}$ (black circles), ${}^{58}\mathrm{Ni}$ (black squares), and ${}^{108}\mathrm{Ag}$ and ${}^{112}\mathrm{Sn}$ (black triangles); nuclei with large neutron excess ${}^{124}\mathrm{Sn}$, ${}^{238}\mathrm{U}$, ${}^{232}\mathrm{Th}$; the crosses correspond to the experiments. The experimental data are taken from Refs. 6, 8–10, 42, 67, and 77–81.

The results are given in Fig. 13. It can be seen that a positive answer to the posed question is possible.

One may also decide on an estimate of the actual production cross sections of the unusual fragments. Naturally, for these estimates it is important to know fragment characteristics such as R_f, $\langle \rho_f \rangle$, the mass, and the spectroscopic data. For ${}^{8}n$, there are theoretical estimates of the quantities needed for this,[101] and they can be used. For ${}^{10}\mathrm{He}$ and ${}^{13}\mathrm{Li}$, there are no suitable data. It is meaningful to vary, for example, R_f and $\langle \rho_f \rangle$. With regard to the spectroscopic data, we assume for ${}^{8}n$ and ${}^{10}\mathrm{He}$ that $S = 0$ and that there are no excited nucleon-stable states. For ${}^{13}\mathrm{Li}$ we assume that $S = \frac{1}{2}$. For the nuclides with $A_f = 10$ and $A_f = 13$, using the existing data[91] for ${}^{10}\mathrm{B}$ and ${}^{13}\mathrm{C}$ and the assumption that $\langle \rho_f \rangle \sim R_f^{-3}$, one can calculate the possible values of $\sigma_f({}^{10}\mathrm{He})/\sigma_f({}^{8}\mathrm{He})$ and $\sigma_f({}^{13}\mathrm{Li})/\sigma_f({}^{11}\mathrm{Li})$ for some values of R_f (Fig. 14). For ${}^{8}n$, the calculation was made for $E_p = 0.7$ GeV and the target nucleus ${}^{238}\mathrm{U}$ with variation in reasonable limits of the values of $\langle \rho_f \rangle$ and R_f (Fig. 15).

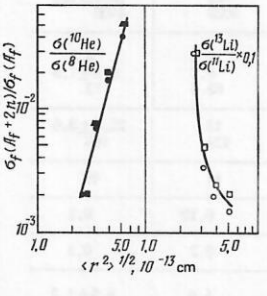

FIG. 14. Dependence of the ratio of the calculated cross sections for production of the fragments ${}^{10}\mathrm{He}$ and ${}^{8}\mathrm{He}$, and ${}^{13}\mathrm{Li}$ and ${}^{11}\mathrm{Li}$ on $\langle r^2 \rangle^{1/2}$ under the assumption that $\langle \rho_f \rangle \sim \langle r^2 \rangle^{-3/2}$. Black circles and open circles are for ${}^{124}\mathrm{Sn}$, black squares and open squares for ${}^{238}\mathrm{U}$, and black triangles for ${}^{232}\mathrm{Th}$; $E_p = 9$ GeV.

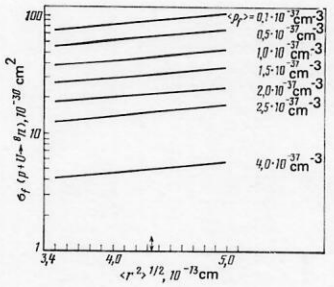

FIG. 15. Calculated dependence of the cross section for production of a ^8n fragment on the values of $\langle \rho_f \rangle$ and $\langle r^2 \rangle^{1/2}$. The arrow on the abscissa indicates the probable value[101] of $\langle r^2 \rangle^{1/2}$ for the ^8n nucleus.

According to Ref. 5, for $E_p = 0.7$ GeV the upper bound for the cross section of the $p + {}^{238}\mathrm{U} \to {}^8n$ reaction is 2.3×10^{-35} cm^2, which is much smaller than the values that follow from Fig. 15. Thus, ^8n nuclei do not exist.

With regard to the nuclides ^{10}He and ^{13}Li, from the existing estimates of the cross sections one cannot make either a positive or a negative assertion about their existence. From this it may be concluded that an experiment with background conditions between one and two orders of magnitude lower than in the previous experiments is needed to decide whether ^{10}He and ^{13}Li exist. We note that the calculated estimates of the ratios $\sigma_f(A_f + 2n)/\sigma_f(A_f)$ for these nuclides are not too small from the point of view of the present-day possibilities of the experimental technique used to investigate fragmentation.[6]

2. HEAVY FRAGMENTS

The data so far accumulated on the production of heavy fragments can provide a basis for attempts to determine the relationship between the mechanisms of formation of light slow fragments and heavy fragments and fission. It is from this point if view that we shall consider them.

Because of the complete absence of models of heavy-fragment production, we shall restrict ourselves to comparing the experimental data on heavy fragments, on the one hand, and on light slow fragments and fission fragments, on the other.

2.1. Excitation functions and isotope distributions for heavy fragments

If we examine Fig. 16, which shows the excitation functions of reactions in which heavy fragments and typical fission fragments are produced, we see that there is a difference between this characteristic and the excitation functions of the reactions in which light slow fragments are produced, namely, for the heavy disintegration products one observes a dependence on the neutron excess of the rate of variation of the cross sections with increasing E_p.

This difference between the characteristics of the production of heavy fragments and fission fragments from the characteristics of the production of light slow

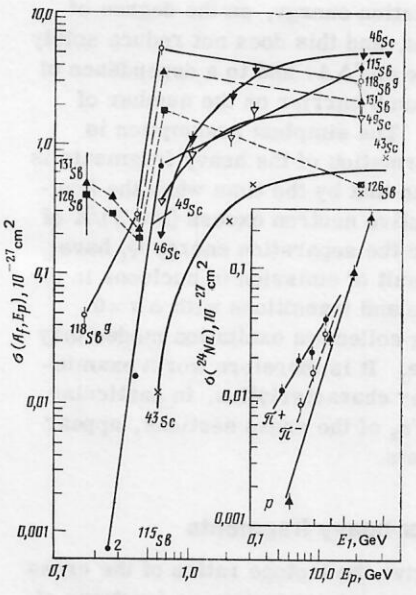

FIG. 16. Excitation functions for the reactions p +U→ ^{j}Sc (continuous curves) and p +U→ ^{j}Sb (broken curves). The inset shows the excitation functions of the reactions $\pi^{\pm}$, p +Au→ ^{24}Na. The experimental data are taken from Refs. 102 and 105.

fragments is more pronounced in the energy dependence of the form of the isotope distributions for the heavy products (Fig. 17). It is interesting that the isotope distributions of the heavy fragments become narrower with increasing E_p, while the distributions of the fission fragments become broader. From the point of view of the model of rapid fragmentation, the change in the isotope distributions cannot be understood if one assumes that $t_f \ll t_n$. In any case, for the heavy fragments and the fission fragments one observes a clear dependence of the cross sections on the "pumping" of

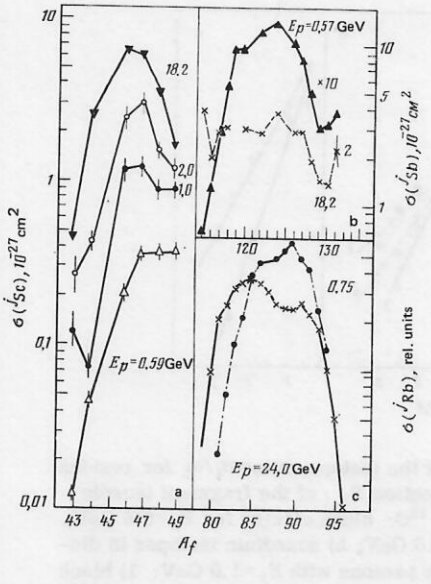

FIG. 17. Isotope distributions for heavy products of uranium disintegration: a) scandium isotopes; b) antimony isotopes; c) rubidium isotopes. The experimental data are taken from Refs. 102–108.

the nucleus with excitation energy, on the degree of breakup of the nucleus, and this does not reduce solely to a linear dependence on $\langle \Delta A \rangle$ and to a dependence of the height of the Coulomb barrier on the number of knocked-out protons. The simplest assumption is that the process of formation of the heavy fragments is drawn out in time, and that by the time when the fragment appears the relative neutron excess $(N-Z)/A$ of the target nucleus and the separation energy Q_f have been changed as a result of emission of nucleons in the pre-equilibrium stage and transitions with $\Delta n = 0$. Naturally, developing collective excitation modes may also have an influence. It is therefore worth examining how more "subtle" characteristics, in particular the isotope ratios σ_1/σ_h of the cross sections, appear for the heavy fragments.

2.2. Isotope ratios for heavy fragments

Figures 7b and 7d give the isotope ratios of the cross sections for heavy-fragment production as functions of $T_{3,f}$. Despite the fact that there are few experimental data, there is a striking similarity to the isotope ratios for light slow fragments in both shape and magnitude. It is very possible that an almost exponential dependence of σ_1/σ_h on $T_{3,f}$ is a characteristic of not only fragments. It can be clearly seen that this is the case in Fig. 18, which shows the isotope ratios of the production cross sections for such nuclides— residual nuclei which are fragments for the breakup of appreciably heavier target nuclei.

The similarity of the form of the dependence on $T_{3,f}$ for light slow fragments, heavy fragments, and residual nuclei may be due to the fact that the cross sections must be determined by the combination $T_{3,f}T'_{0,3}/A'_0$, where $T'_{0,3}$ is the third projection of the isospin of the product that makes up the observed product A_f to the decaying nucleus A'_0.

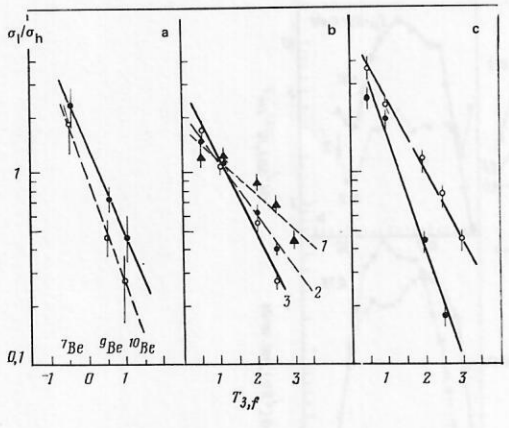

FIG. 18. Dependence of the isotope ratios σ_1/σ_h for residual nuclei on the third projection $T_{3,f}$ of the fragment isospin: a) target nuclei ^{12}C and ^{13}O: black circles for $E_p = 0.6$ GeV, open circles for $E_p = 0.15$ GeV; b) scandium isotopes in disintegrations of nuclei by protons with $E_p = 1.0$ GeV: 1) black triangles for ^{60}Ni and ^{62}Ni, 2) black circles for ^{58}Ni and ^{60}Ni, 3) open circles for ^{54}Fe and ^{56}Fe ($\Delta N = 2$); c) open circles for ^{70}Ge and ^{76}Ge, black circles for ^{58}Ni and ^{64}Ni. The experimental data are taken from Refs. 109 and 110.

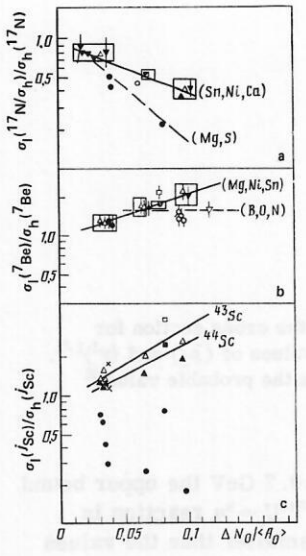

FIG. 19. Dependence of the isotope ratios σ_1/σ_h on the mean neutron excess $\Delta N/\langle A_0 \rangle = (N_h - N_1)/\frac{1}{2}(A_h + A_1)$ of the target nuclei: a) $A_f = {}^{17}N$, target nuclei: black circles for $^{24,25,26}Mg$, open circles for $^{32,34}S$, black triangles for $^{40,44}Ca$, open triangles for $^{58,60,62,64}Ni$, black inverted triangles for $^{112,116,119,120,122,124}Sn$; b) $A_f = {}^{7}Be$; c) $A_f = {}^{43}Sc$, ^{44}Sc, black circles for ^{47}Sc, target nuclei: open triangles for $^{58,60,62,64}Ni$, crosses for $^{54,56}Fe$, open squares for $^{70,76}Ge$. For clarity, the points satisfying the condition $A_f \lesssim A_0/3$ are enclosed in rectangles. The experimental data are taken from Refs. 10, 11, 42, 50, and 109–115.

If this is correct, there must a difference in the dependence of σ_1/σ_h on $y = \Delta N/\langle A_0 \rangle$ ($\Delta N = N_{0,h} - N_{0,l}$, $2\langle A_0 \rangle = A_{0,h} + A_{0,l}$) in the cases when the product A_f is a fragment and when it is a residual nucleus produced in the final stage of the evolution. Figure 19 gives examples of the dependence of σ_1/σ_h on y for ^{7}Be, ^{17}N, $_{j}Si$ In fact, the difference between the y dependence of the ratios σ_1/σ_h is very appreciable. For the light slow fragments, the dependence of σ_1/σ_h on y is fairly close to exponential, and the total dependence of σ_1/σ_h on $T_{3,f}$ and $\Delta N/\langle A_0 \rangle$ can be well approximated by the relation

$$\sigma_1/\sigma_h \sim \exp[-bT_{3,f}T_{3,0}/\langle A_0 \rangle]. \qquad (25)$$

The exponential dependence on $T_{3,0}/\langle A_0 \rangle$ of the ratios σ_1/σ_h for the heavy fragments can be clearly seen in Figs. 7b and 7d, the parameter b in the approximating curve being the same as for the light slow fragments. The attempt to calculate the behavior of σ_1/σ_h as a function of y for the tin isotopes (Fig. 20) in the framework of the model of rapid fragmentation with $t_f < t_n$ does not lead to success. However, if one assumes that by the time of formation of the heavy fragments the shell effects are already weakened to a considerable degree and that Q_f is determined by the values of the masses in the liquid-drop model for the decaying nucleus and the "residual" nucleus, then the calculated curve $\sigma_1/\sigma_h = f(y)$ almost coincides with the continuous curve in Fig. 20a. Without according too serious a meaning to this fact, we nevertheless note that the existing data on σ_1/σ_h for heavy fragments agree well

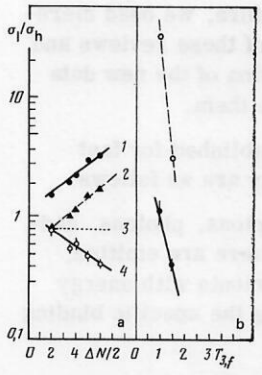

FIG. 20. Dependence of the isotope ratios σ_l/σ_h for the heavy fragments ^{17}N and ^{24}Na on $\Delta N = N_h - N_l$ (a) and on $T_{3,f}$ (b). The points with error bars are the experimental values; 1) calculation of σ_l/σ_h in the framework of the model of Ref. 82 (black symbols); 2) the same group of points with normalization to the isotope ratio σ_l/σ_h for $\Delta N = 2$; 3) calculation in accordance with the model of pre-equilibrium fragmentation (Sec. 1.4) under the assumption of "fast fragmentation"; 4) straight line passing through the experimental points (open symbols): calculation in the framework of the model of pre-equilibrium fragmentation under the assumption that the shell corrections for the masses of the target nucleus and the residual nucleus are "switched off."[11] In Fig. 20b the open circles are the results of calculation in themodel of pre-equilibrium fragmentation.

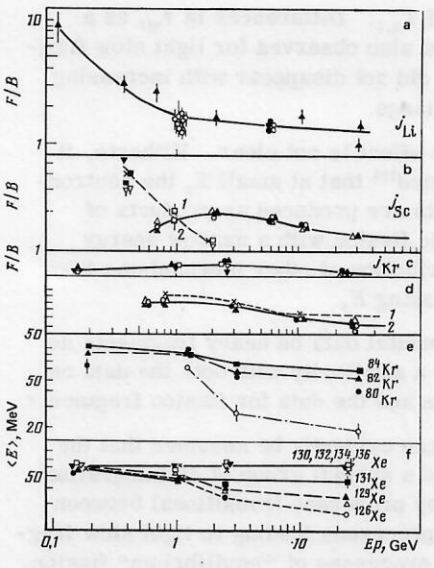

FIG. 21. Some kinematic characteristics of the fragments: a) the angular anisotropy F/B for lithium isotopes; b) the angular anisotropy F/B for heavy fragments (the broken and continuous curves join the points corresponding to the data for reactions induced by fast nuclei and protons, respectively; the points 1 and 2 for $E_p = 1.0$ GeV are the data for the isotopes ^{124}Sn and ^{112}Sn, the fragment ^{24}Na); c) the angular anisotropy for the "fragments" ^{j}Kr in p+Th reactions; d) values of the mean energy $\langle E \rangle$ for heavy fragments in the form of scandium isotopes (continuous curve) and values of the effective Coulomb barrier (broken curve). The reaction p +U→ ^{j}Sc; e) the values of $\langle E \rangle$ for krypton isotopes as fission fragments. The reaction p +Th→ ^{j}Kr; f) the values of $\langle E \rangle$ for xenon isotopes as fission fragments. The reaction p +Th→ ^{j}Xe. The experimental data are taken from Refs. 42, 48, 49, 77–81, 95, 102, 104, 116–120, and 121.

with the assumption that they are formed at a deeper stage of the relaxation but nevertheless before nucleon emission has strongly changed the third projection of the isospin of the relaxaing nucleus. It is possible that with increasing A_f there would in such a case be some matching of the characteristics of the production of the heavy fragments and fission fragments. The experiments give some support to this suggestion.

In particular, as is shown in Ref. 134 for fission reactions, shell effects must be "switched off" in the deep stages of the relaxation of the cascade-excited nuclei to achieve better agreement with experiment.

2.3. Angular distributions and spectra of heavy fragments

One of the important characteristics of the angular distributions is the s-called forward–backward anisotropy F/B, i.e., the ratio of the number of particles emitted in the forward (i.e., in the direction of the beam) hemisphere. For light slow fragments, the dependence of F/B on E_p is well known (see, for example, Refs. 42, 43, 77, and 78): F/B decreases with increasing E_p, approaching unity.

Examining Fig. 21, we see that for the heavy fragments and fission fragments the behavior of F/B is different. Between $E_p = 1$ GeV and $E_p = 3$ GeV, the function $f(E_p) = F/B$ passes through a maximum, and the values of $f(E_p)$ for the heavy fragments are somewhat greater than for the fission fragments. For bombardment of nuclei by nuclei A_1, the values of F/B for the same value of E_1 are greater than for bombardment by protons.

It is interesting that a similar effect holds for light slow fragments.

In Ref. 118, the similarity in the behavior of F/B for ^{24}Na and ^{28}Mg heavy fragments and for fission fragments was interpreted as a manifestation of general features of their production mechanism. A confirmation of this was seen, for example,[118] in the dependence on E_p and the mean energy $\langle E \rangle$ of the heavy fragments and fission fragments (for example, in Fig. 21).

However, the decrease in $\langle E \rangle$ for heavy fragments with increasing E_p is similar to the decrease in the height of the Coulomb barrier with increasing E_p due to knockout of nucleons, and it may be basically determined by this effect. We note that this effect also has an analogy in the data on $E_{m.p}$ for light slow fragments (see Table II).

More interesting are the data obtained in Ref. 121 on the dependence of the shape parameters of the heavy-fragment spectra on E_p (in particular, τ_{eff} when the spectra are approximated by the MRI formulas). It was found that for relatively small E_p ($E_p \leq 1$ GeV) the value of τ_{eff} for neutron-rich heavy fragments is approximately two times smaller than for neutron-deficient fragments. With increasing E_p, this difference decreases, and at large E_p we have $\tau_{eff} \approx 20$

MeV irrespective of $T_{3,t}$. Differences in τ_{eff} as a function of $T_{3,t}$ were also observed for light slow fragments,[42,98] but they did not disappear with increasing E_p and were not so large.

The nature of this effect is not clear. Hitherto, it has only been assumed[121] that at small E_p the neutron-rich heavy fragments are produced as products of strongly asymmetric fission with a narrow energy spectrum, the contribution of other mechanisms increasing with increasing E_p.

Thus, the experimental data on heavy fragments do indeed demonstrate a similarity with both the data on light slow fragments and the data for fission fragments.

On this basis, it can evidently be assumed that the heavy fragments are a special group of disintegration products produced by processes transitional between the fast production processes leading to light slow fragments and the slow processes of "equilibrium" fission. If this is indeed the case, data on heavy fragments could provide helpful information on the development of collective processes in nuclei in the pre-equilibrium stage, this, of course, requiring appropriate theoretical models.

3. FAST FRAGMENTS

The experimental data considered in the previous sections relate to the interaction stage that corresponds to decay of the excited nucleus. Although it is not yet entirely clear what physical processes are taking place, the empirical laws governing the production of light slow fragments are clear. Whether they are formed from nucleons of the exciton gas[44] or from nucleons of the nucleus near the Fermi surface under the influence of local density defects[46]—these are interesting questions but hardly of fundamental importance. The value of an answer to them would consist in the possibility of solving a number of problems of nuclear kinetics and nuclear structure of the basis of customary ideas about the nucleus.

The physics of fast fragments is a different matter. The interest in them, as in other cumulative particles, is due to the part they play in the solution of fundamental problems of strong-interaction physics (Refs. 15, 16, 26, 39, and 40). In this connection, it is sufficient to recall that the production of fast fragments is associated with the possible existence of objects such as fluctons[15,16,39,40] and nuclear fireballs.[12-14] There are some, it is true, more modest hypotheses—for example, the coalescence hypothesis.[17,18,22] What actually happens is at present very difficult to say, but the experimental investigations are developing, and their data can already be compared with the simplest variants of the models in the framework of the mentioned hypotheses.

In the Introduction we noted that there are fairly complete reveiws (Refs. 15, 16, 26, 39, and 40) of the physics of fast fragments, these describing both the experimental data, which were largely obtained at the end of the seventies, and attempts at their model interpretation (usually in the framework of variants of the "flucton" model[15,16,40]). Therefore, we need merely briefly summarize the contents of these reviews and turn to a consideration and discussion of the new data and some other attempts to analyze them.

The basic experimental facts established for fast fragments with reasonable certainty are as follows:

1. When particles of any type (leptons, photons, hadrons, nuclei) interact with nuclei there are emitted, together with other particles, fragments with energy (per nucleon) appreciably exceeding the specific binding energy of the fragment.

2. The invariant cross sections $E_0 d^3\sigma/d^3p$ for production of fast fragments can be represented by the expressions (Refs. 16, 26, 34, and 38)

$$E_0\frac{d^3\sigma}{d^3p}=C_1\exp(-Bp^2); \tag{26'}$$

$$E_0\frac{d^3\sigma}{d^3p}=C_2\exp(-E/T_0); \tag{26''}$$

$$E_0\frac{d^3\sigma}{d^3p}=C_3\exp(-p/P_0), \tag{26'''}$$

where E_0 is the total energy of the fragment, p is its momentum, and C_j, B, T_0, P_0 are parameters.

The choice of the most convenient representation of the invariant cross section is as yet a subject of discussion, and the relations (26) do not exhaust the employed approximations.

3. The invariant cross sections are increasing functions of the energy E_1 of the bonbarding hadrons and nuclei, but in the region of relativistic energies E_1 they reach a plateau. The energy at which the cross sections cease to increase is different for different target nuclei and larger, the larger the mass number A_0.

4. With increasing A_0, the slope parameter B decreases (T_0 and P_0 increase accordingly) when nuclei are bombarded by hadrons.[16,26,34] At high E_1, the slope parameters depend weakly on A_0 and on the species of the bombarding particles.

5. The cross sections can be assumed to be proportional to A_0^N, where N depends on the species of the bombarding particle, A_t, E, and E_1.[16,26,34] Investigations were made into the dependence of the parameters used to approximate the cross sections on the fragment detection angles θ.[16,26,34] It was found that the parameters T_0 increase somewhat with increasing $\cos\theta$ (B decreases accordingly).

Particular attention was paid to the parameter N in the A_0 dependence, which, according to the established opinion (see Refs. 16, 22–27, 34, 39, and 122), gives the clearest information about the types of processes leading to the production of fast fragments.

Further experimental study of the production of fast fragments made it possible to confirm and make more accurate the previously obtained data[34-39,67] with a view of establishing the production mechanism of the cumulative particles, including fast fragments. This revealed facts that are rather interesting and unexpected from the point of view of models of both types.

These data, and also their phenomenological analysis, are briefly discussed below.

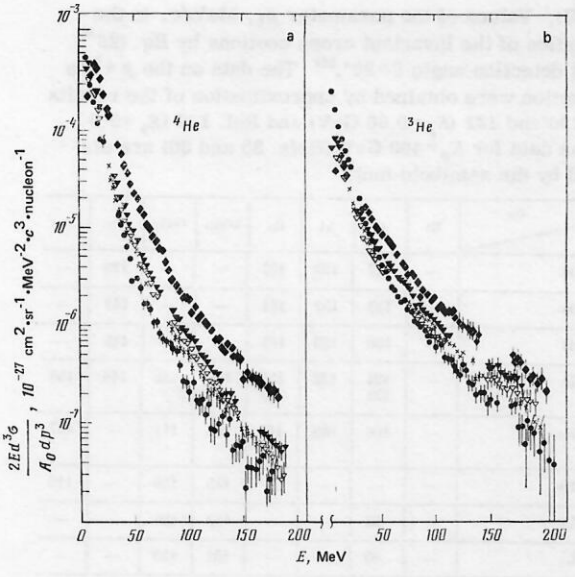

FIG. 22. Spectra of fragments resulting from bombardment of nuclei with protons with $E_p = 6.7$ GeV, $\theta = 90°$; target nuclei: ^{12}C (black circles), Cu (crosses), ^{112}Sn (black triangles), ^{124}Sn (open triangles) and Au (black diamonds).

Interesting results on fast fragments were obtained by the groups of the Radium Institute[27,37,38,67] and the ITEF (Institute of Theoretical and Experimental Physics)–Pennsylvania Collaboration.[35,36] Figure 22 shows examples of the invariant cross sections of fast-fragment production on the nuclei C, Cu, ^{112,124}Sn, Au following bombardment with 6.7-GeV protons. Two circumstances are to be noted. First, as for light slow fragments, the slopes of the ^{3}He$_2$ spectra are smaller than for ^{4}He$_2$. Second, the higher the mass number of the target nucleus, the higher the curve of the corresponding invariant cross section $E_0 d^3\sigma/(A_0 d^3p)$ (normalized to A_0). This indicates a very strong A_0 dependence of the cross sections.

The experimental sequence of values of the exponent N for different fragments[26] in $p + A_0$ reactions was noted long ago: $N(p) = 4/3$, $N(d) = 5/3$, $N(t) = 2$.

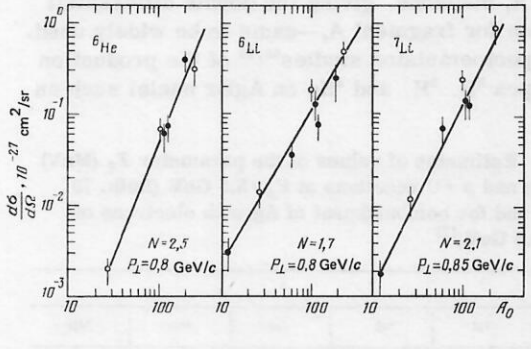

FIG. 23. Dependence of the differential cross sections on A_0 for the fragments ^{6}He, ^{6}Li, and ^{7}Li. The values of the parameter N in the approximation of the A_0 dependence of the cross sections by the expression $\sigma_f \sim A_0^N$ are given together with the "mean values" of the momentum $p_\perp/A_f$, $\theta = 90°$, $E_p = 6.7$ GeV. The data are taken from Ref. 38.

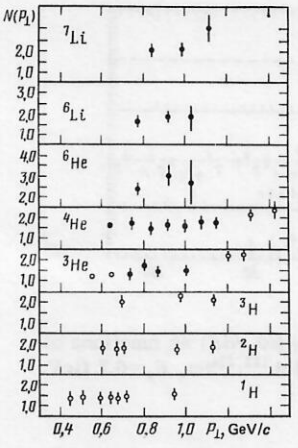

FIG. 24. Dependence of the parameter N on $p_\perp$. The data are taken from Ref. 38.

A new result is that experiment (we are speaking about fragment yields at $\theta = 90°$ (Ref. 38)) reveals a very weak dependence of N on the momentum $p_\perp$ for $p_\perp > 0.5$ GeV/c and a strong dependence on the fragment isospin $T_{3,f} = (N_f - Z_f)/2$. This is illustrated by Figs. 23 and 24 and Table VI. A model calculation made in the framework of the ideas of modern relativistic nuclear physics[39] gives, as follows from Table VI, some different values of the parameter N and, which is more important, values that do not depend on $T_{3,f}$.

Examining Fig. 25, we can see one further interesting effect: For the target isotopes ^{112}Sn and ^{124}Sn there is a dependence of the fast-fragment production cross sections on the isospin $T_{3,f}$ of the target nucleus that in general repeats what was observed for light slow fragments. It is found that for the fast fragments ^{3}He, ^{4}He, ^{6}Li, ^{7}Li the yields from the light isotope are larger than those from the heavy, while for ^{6}He it is the opposite. The previous results on theyields of protons and deuterons from isotope nuclei did not reveal a clear dependence of the cross sections on the neutron excess $N_0 - Z_0$ of the target nucleus.

As follows from Fig. 24, the exponent N can be assumed to be almost independent of the fragment energy E (or, at the least, to increase weakly with increasing E). It is interesting that in experiments on electroproduction of fast fragments[122] (at $E_p = 4.5$ GeV) an increase in N with increasing A_f was noted, and a decrease with increasing energy E of the fragment. For example, for ^{4}He the value of N changes as E is in-

TABLE VI. Values of the exponent N for the A_0 dependence of the cross sections for production of fast fragments when $E_p \geq 6.7$ GeV. Comparison with the model prediction of Refs. 26 and 39. The experimental data are taken from Refs. 6, 7, 35, and 36.

A_f	^{1}H	^{2}H	^{3}H	^{3}He	^{4}He	^{6}He	^{6}Li	^{7}Li
Model prediction	1.0	1,3	1,7	1,7	2,0	2,7	2,7	3,0
Experiment	1.3	1,8	2,1	1,5	2,0	2,7	1,9	3,0

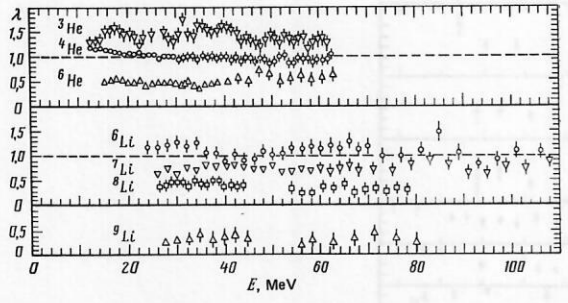

FIG. 25. Isotope ratios $\lambda=(d\sigma_1/dE)/(d\sigma_h/dE)$ as functions of the fragment energy E. Target nuclei ^{112,124}Sn, $E_p=6.7$ GeV. The data are taken from Ref. 67.

creased from 40 to 68 MeV from about 2.3 to about 1.65 (the data are taken from the graph of Ref. 122). At the same time, the values of N for ^{3}He and ^{3}H are very different: $N\approx 2.2$ for ^{3}He at energy $E\approx 30$ MeV, while $N\approx 1.5$–1.55 for tritons at the same energy, i.e., the picture is the opposite of what is reflected in Table VI for interactions initiated by relativistic protons. The differences between the values of N for the reactions with protons and electrons are not unexpected.[16,123] Unexpected is the opposite behavior of the dependence of N on $T_{3,t}$ for nuclides with $A_t=3$.

Completing our discussion of the features of the experimental A_0 dependences of the fast-fragment production cross sections, we give Fig. 25, which shows the dependence on the fragment energy of the ratios of the fragmentation cross sections on the ^{122}Sn and ^{124}Sn nuclei[67] at $E_p=6.7$ GeV. The analogous ratios[98] for $E_p=0.66$ GeV demonstrated a rapid (already at $E\approx 10$ MeV/nucleon) disappearance of the isotope effect for the cross sections. The data in Fig. 25 indicate rather that in this case the isotope effect has a weaker dependence on E.

Interesting new data are those on the dependence of the shape parameters of the fragment spectra on the properties and energy of the bombarding particles and on the characteristics of the fragment and target nucleus. To discuss this question, we must consider the corresponding approximation of the spectra. For the approximation (26‴) at $E_p=6.7$ and 400 GeV (fragment detection angle 90°) the values of the parameter P_0 were obtained (Table VII). Except for the case of ^{4}He production on Al nuclei ($E_p=400$ GeV) the following may be noted. For the lightest fragments, one observes, in general, a weak growth of P_0 with increasing A_0, i.e., the spectra become somewhat "harder." For heavier fragments, this effect becomes particularly noticeable. In experiments on electroproduction of fast fragments the dependence of the shape of the fragment spectrum on the mass number of the fragment and on its isospin $T_{3,t}$ was also investigated.[122] To analyze the spectra, the approximation (26″) was used. The obtained values of T_0 for the target nuclei ^{9}Be ^{108}Ag, and Au revealed the presence of an A_0 dependence of this parameter. The values of T_0 for deuterons and tritons are 5–7 and 8–7 MeV in the range of A_0 from 9 to 197. In Ref. 122 the values of T_0 for the fragment spectra

TABLE VII. Values of the parameter p_0, MeV/c, in the approximation of the invariant cross sections by Eq. (26‴). Fragment detection angle $\theta=90°$.[141] The data on the $p+^9$Be $\rightarrow$ ^{8}Li reaction were obtained by approximation of the results of Refs. 130 and 131 ($E_p=0.66$ GeV) and Ref. 133 ($E_p=9.0$ GeV). The data for $E_p=400$ GeV (Refs. 35 and 36) are distinguished by the semibold font.

A_f \ A_0	Be	C	Al	Cu	^{112}Sn	^{124}Sn	Ta	Au
^{1}H	—	**117**	**122**	**127**	—	—	**128**	—
^{2}H	—	**139**	**152**	**161**	—	—	**147**	—
^{3}H	—	**138**	**123**	**142**	—	—	**146**	—
^{3}He	—	**121** **122**	**132**	**153** **133**	**129**	**135**	**148**	**156**
^{4}He	—	**106**	**168**	**144** **113**	**105**	**111**	—	**127**
^{6}He	—	—	—	—	**125**	**126**	—	**110**
^{6}Li	—	**92**	—	—	**132**	**136**	—	—
^{7}Li	—	**89**	—	—	**131**	**130**	—	—
^{8}Li 9.0 GeV	**84,0**	—	—	—	—	—	—	—
^{8}Li 0.66 GeV	**72,5**	—	—	—	—	—	—	—

were calculated for the same range of energies of the secondary particles using the data of Refs. 79 and 80 at $E_p=5.5$ GeV (Table VIII). For the hydrogen isotopes, one observes a difference between the T_0 values for electroproduction of fragments and for bombardment of nuclei with protons, while for the helium isotopes the T_0 values agree somewhat better.

These experimental data refer to a fairly narrow part of the fragment energy spectrum, and they need to be made more accurate and extended.

At the present time, wide use is made of a representation of the experimental data in a form that derives from the Butler–Pearson model,[17] in which the formation of fast fragments is regarded as a process of pairing of fast nucleons, the energy and momentum excess being passed over to the nucleus by interaction with the average nuclear field. This model did not give perfect agreement with experiment,[17] but one of its features—the factorization of the double differential cross sections of A_t nucleons, giving the double differential cross section for fragment A_t—came to be widely used. Already in photoemulsion studies[32,33] of the production of the isotopes ^{2}H, ^{3}H, and ^{3}He on AgBr nuclei such an

TABLE VIII. Estimates of values of the parameter T_0 (MeV) for the p +Ag and p +U reactions at $E_p=5.5$ GeV (Refs. 79, 80, and 122) and for bombardment of Ag with electrons of energy $E_e=4.5$ GeV.[122]

A_1+A_0	A_f				
	^{1}H	^{2}H	^{3}H	^{3}He	^{4}He
p+U	10	11	10	21	11
p+Ag	12	13	14	21	15
e+Ag	~4	~6	~7.5	~20	~17

approach was successfully used to describe the fast-fragment spectra on the basis of the proton spectra. Indeed, the first major success in such an approach was acheived by Poskanzer's group,[22] who showed that by factorizing the nucleon double differential cross sections in the case of bombardment of uranium nuclei with relativistic nucleons and nuclei one can give a very good description of the experimental double differential cross sections of light fast fragments. One introduces phenomenologically an adjustable parameter P_0, which is associated with the size of the region of momentum space within which nucleons will coalesce. This empirical model—the "coalescence model"—was also used to analyze a large body of experimental data on fast-fragment production on nuclei bombarded with relativistic particles in the experiments of the ITEF-Pennsylvania[35,36] and Radium Institute[67] groups. The mean value of P_0 is about 190 MeV/c, which is close to the result of Ref. 124 for nucleus–nucleus interactions ($P_0=200$ MeV/c). This suggested[67] that the mechanism of fast-fragment production is the same in interactions of nucleons and of nuclei with nuclei.

Figure 26 gives examples of the description of the structure function

$$\rho(p)=\frac{E_0}{\sigma_{\text{in}}(A_1+A_0)}\frac{d^3\sigma_f}{d^3p} \tag{27}$$

in the framework of the phenomenological coalescence

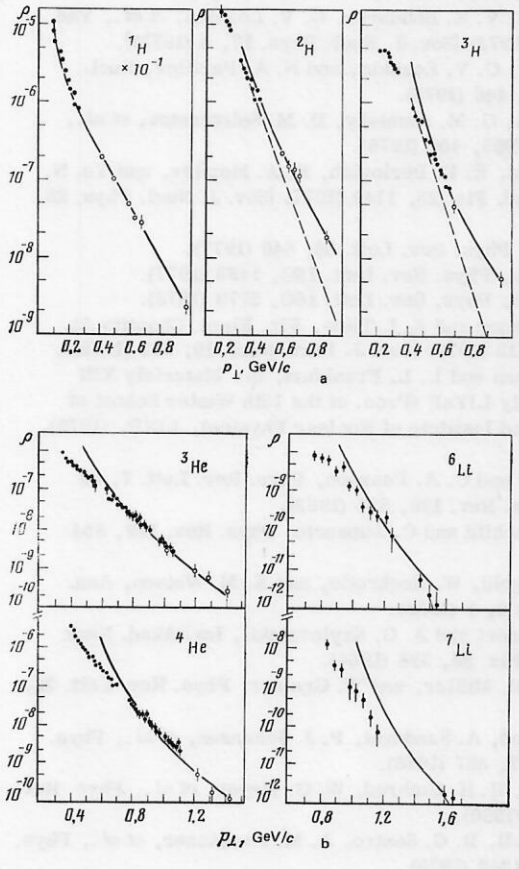

FIG. 26. Comparison with the predictions of the phenomenological coalescence model of the experimental data on the fragment spectra, $\theta=90°$, $E_p=6.7$ GeV.[133]

model. It can be seen that on the basis of the nucleon spectrum $E_0 pd^3\sigma/d^3p$ one can, using the relation

$$E_{0,A_f}d^3\sigma_f/d^3p=\frac{1}{A_f^3N_f!\,Z!}\left(\frac{N_0}{Z_0}\right)^{N_f}\left(\frac{4\pi}{3}\frac{p_0^3}{\sigma_{\text{in}}(A_1+A_0)M_p}\right)^{A_f-1}\times\left[\frac{E_{0,p}}{A_f}\frac{d^3\sigma(p/A_f)}{d^3p}\right]^{A_f},\quad p_0=190\,\text{MeV}/c, \tag{28}$$

reproduce well the double differential cross section in the high-momentum part of the spectrum even for complicated fragments like the lithium isotopes. This enables us to regard (28) with some confidence as an approximation of the experimental data, although its physical content requires elucidation, especially in view of the fact that the systematization (28) explicitly—if there really is coalescence of the nucleons—presupposes identity of the spectra of the fast neutrons and protons. The experiments do not give particular reasons for assuming these spectra to be the same.

Fairly often the experimental data on fast fragments are discussed in the framework of the nuclear-fireball model, in the version of it usually associated with Mekjian's paper of Ref. 12. Applied to the fragmentation problem, this model has the following content: There exist some mechanism by which a large number of nucleons are brought to interact, thermodynamic and "chemical" equilibrium being established between them as a result of elastic and inelastic processes (including coalescence into light nuclei). This hypothesis in conjunction with the ideal-gas model, which gives the distribution functions of the particles with respect to the energies and in terms of the chemical potential with respect to the species, makes it possible to obtain estimates of the shape of the spectra and the absolute cross sections for the production of different interaction products. The paraneters of the model are the temperature τ_0, which is usually determined from the spectrum, the critical matter density ρ_c of the expansing fireball at which the composition is already assumed to be established, the spectrum, and the translational velocity of the fireball's center of mass.

Analysis of Mekjian's model (see, for example, Refs. 13, 130, and 135) showed that $\rho_c\approx 0.3\rho_0$, where ρ_0 is the ordinary density of nuclear matter, τ_0 is of the order of 50 MeV, and the conditions for the attainment of thermodyanmic and "chemical" equilibrium are determined by the densities ρ_i of the particles of different species and by their interaction cross sections (for thermodynamic equilibrium by the elastic σ_{ij}^{el}, and for "chemical" equilibrium by the corresponding inelastic σ_{ij}^{in}). It was found that thermodynamic equilibrium can occur for $\sigma_{ij}^{\text{el}}\approx(25-100)\times10^{-27}$ cm^2, and that it may be attained more rapidly than the fireball expands. The conditions for attainment of chemical equilibrium are more difficult. In Tables IX and X we have collected together some results of analysis of the experimental data in the framework of this model, giving an idea of the typical values of its parameters. Since this model did not have a good description of the experimental data overall, there was proposed a "firestreak" model (for example, in Ref. 131), in which the fireball is regarded as consisting of layers of particles produced at

TABLE IX. Parameters of the fireball model for the ^{20}Ne (0.4 GeV/nucleon)+U→A_f reaction. Two sources are taken into account: a "thermal" one with velocity $\beta_2 c$ and temperature τ_2 and the fireball with velocity $\beta_1 c$ and temperature τ_1.[54]

A_f	β_1	τ_1, MeV	β_2	τ_2, MeV	fireball yield / total yield
^1H	0.27	49	0.078	26	0.53
^2H	0.27	49	0.083	26	0.24
^3H	0.27	49	0.079	24	0.13
^3He	0.27	49	0.15	49	0.11
^4He	0.27	49	0.10	36	0.12
^8Li	0.27	49	0.052	35	0.041
B	0.27	49	0.073	56	0.017
C	0.27	49	0.080	62	0.016

different impact parameters b. In the layers, equilibrium is assumed. As is shown in Ref. 124, the firestreak model gives a poorer description of the experiments than that of the phenomenological coalescence model.

CONCLUSIONS

It is at present not possible in the framework of a brief review to give a complete survey of the results of fragmentation investigations. The material we have selected, while naturally reflecting to some extent the author's interests, can nevertheless give an idea of this rapidly developing branch of physics.

Irrespective of the extent to which the pre-equilibrium fragmentation models are correct, they can be regarded as phenomenological systematizations of the data. On their basis, there has been a gradual clarification of the connections between the characteristics of the target nuclei, the fragments, and the cascade process and the characteristics of the production of light slow fragments, and one can at least qualitatively understand some features of the productionof heavy fragments.

It is found that in the region of intermediate energies one can, in the framework of a cascade model that includes pre-equilibrium decay, give a unified description of the main data on the nucleon and meson components,[43] the residual nuclei (see, for example, Refs. 43 and 132), the fission fragments (see, for example, Refs. 43 and 134), and fragments. Not yet encompassed are the more "rare" phenomena—cumulative production of mesons and nucleons and, possibly, the production of fast fragments, though in this last case too one finds a formal connection between the characteristics of the fast nucleon component and the fragments, i.e., there is a possibility of relating the data on the fast fragments to a cascade process.

TABLE X. Calculated properties of fireball for the value of the impact parameter b having the maximal statistical weight ($b = b_m$), the A_1+U→A_f reaction.[28]

A_1	E_1, GeV/nucleon	b_m, 10^{-13} cm	Number of nucleons N	τ_0, MeV	β
^{20}Ne	0.25	4.8	64	28	0,22
^{20}Ne	0.40	4.8	64	47	0,27
^4He	0.40	4.7	25	33	0,17
^{20}Ne	2.1	4.8	64	92 *	0,56

*Excited baryon states are taken into account.

On the basis of the available experimental data and their systematizations it may be concluded, with due care, that the nature of the fragmentation phenomenon will already be understood in a few years. This will provide the solution to one of the oldest problems of nuclear physics.

But for this it will evidently be necessary to increase appreciably the accuracy of the experiments, including the measurement of the excitation functions, and to make experiments on a large number of monoisotopic targets, including targets for which the shell effects in the masses of the nuclei and in the values of g are appreciable.

I am grateful to O. V. Lozhkin and L. Kh. Batist for collaborating with me in investigating some of the questions discussed in the present review.

[1]O. V. Lozhkin and A. A. Rimskiĭ-Korsakov, Zh. Eksp. Teor. Fiz. 40, 1519 (1961) [Sov. Phys. JETP 13, 1064 (1961)].
[2]R. Klapisch, C. Thibault, A. M. Poskanzer, *et al.*, Phys. Rev. Lett. 29, 1254 (1972).
[3]A. M. Poskanzer, S. W. Cosper, E. K. Hyde, and J. Cerny, Preprint UCRL-17267, Berkeley (1966).
[4]C. Detraz, Phys. Lett. B66, 333 (1977).
[5]A. Turkevich, J. R. Cadieux, J. Warren, *et al.*, Phys. Rev. Lett. 38, 1129 (1977).
[6]V. I. Bogatin, E. A. Ganza, O. V. Lozhkin, *et al.*, Yad. Fiz. 32, 27 (1980) [Sov. J. Nucl. Phys. 32, 14 (1980)].
[7]C. Thibault-Philippe, Thesis [in French], Faculté des Sciences d'Orsay, Ser. A, No. 783, Orsay (1971).
[8]V. I. Bogatin, V. K. Bondarev, O. V. Lozhkin, *et al.*, Yad. Fiz. 17, 9 (1973) [Sov. J. Nucl. Phys. 17, 4 (1973)].
[9]V. I. Bogatin, O. V. Lozhkin, and N. A. Perfilov, Nucl. Phys. A206, 446 (1976).
[10]E. N. Volnin, G. M. Amalsky, D. M. Seliverstov, *et al.*, Phys. Lett. B55, 409 (1975).
[11]L. Kh. Batist, É. E. Berlovich, K. A. Mezilev, and Yu. N. Novikov, Yad. Fiz. 25, 1140 (1977) [Sov. J. Nucl. Phys. 25, 605 (1977)].
[12]A. Mekjian, Phys. Rev. Lett. 38, 640 (1977).
[13]J. I. Kapusta, Phys. Rev. Lett. 16C, 1493 (1977).
[14]S. Das Gupta, Phys. Rev. Lett. 18C, 2773 (1978).
[15]V. K. Luk'yanov and A. I. Titov, Fiz. Elem. Chastits At. Yadra 10, 815 (1979) [Sov. J. Part. Nucl. 10, 321 (1979)].
[16]M. I. Strikman and L. L. Frankfurt, in: Materialy XIII zimneĭ shkoly LIYaF (Proc. of the 13th Winter School of the Leningrad Institute of Nuclear Physics), LINP, (1979), pp. 137–191.
[17]S. T. Butler and C. A. Pearson, Phys. Rev. Lett. 7, 69 (1961); Phys. Rev. 129, 836 (1963).
[18]A. Schwarzschild and C. Zupancic, Phys. Rev. 129, 854 (1964).
[19]A. E. Glassgold, W. Heckrotte, and X. M. Watson, Ann. Phys. (N.Y.) 6, 1 (1959).
[20]L. P. Rappoport and A. G. Krylovetskiĭ, Izv. Akad. Nauk SSSR, Ser. Fiz. 28, 388 (1964).
[21]W. Scheid, H. Müller, and W. Greiner, Phys. Rev. Lett. 32, 741 (1974).
[22]H. H. Gutbrod, A. Sandoval, P. J. Johansen, *et al.*, Phys. Rev. Lett. 37, 667 (1976).
[23]A. Sandoval, H. H. Gutbrod, W. G. Meyer, *et al.*, Phys. Rev. C 21, 1321 (1980).
[24]G. D. Westfall, R. G. Sextro, A. M. Poskanzer, *et al.*, Phys. Rev. C 17, 1368 (1978).
[25]W. G. Meyer, H. H. Gutbrod, Ch. Lukner, and A. Sandoval, Phys. Rev. C 22, 179 (1980).
[26]V. S. Stavinskiĭ, Fiz. Elem. Chastits At. Yadra 10, 949

(1979) [Sov. J. Part. Nucl. 10, 373 (1979)].
[27]V. I. Bogatin, E. A. Ganza, O. V. Lozhkin, *et al.*, Yad. Fiz. 32, 1363 (1980) [Sov. J. Nucl. Phys. 32, 703 (1980)].
[28]J. Gosset, H. H. Gutbrod, W. G. Meyer, *et al.*, Phys. Rev. C 16, 629 (1977).
[29]A. M. Poskanzer, R. G. Sextro, A. M. Zebelman, *et al.*, Phys. Rev. 35, 1701 (1975).
[30]V. G. Bogdanov, N. A. Perfilov, V. A. Plyushchev, and Z. I. Solov'eva, Preprint RI-92 [in Russian], V. G. Khlopin Radium Institute, Leningrad (1975).
[31]J. A. Gaidos, L. J. Gutay, R. Mitchell, *et al.*, Phys. Rev. Lett. 42, 82 (1979).
[32]M. Zafar, M. Irfan, I. Achmad, *et al.*, Nuovo Cimento 20A, 354 (1974).
[33]M. Zafar, M. Irfan, K. B. Lah, *et al.*, Nuovo Cimento 24A, 111 (1974).
[34]A. M. Baldin, V. K. Bondarev, *et al.*, Soobshchenie (Communication) RI-11302, JINR, Dubna (1978).
[35]Yu. D. Bayukov *et al.*, Yad. Fiz. 33, 183 (1981) [Sov. J. Nucl. Phys. 33, 94 (1981)].
[36]S. Frankel, V. Frati, M. Gassaly, *et al.*, Phys. Rev. C 20, 2257 (1979).
[37]A. Yu. Murin, V. I. Bogatin, E. A. Ganza, *et al.*, Preprint RI-138 [in Russian], V. G. Khlopin Radium Institute, Leningrad (1980).
[38]V. I. Bogatin, E. A. Ganza, O. V. Lozhkin, *et al.*, Preprint 1-81-106 [in Russian], JINR, Dubna (1981).
[39]A. M. Baldin, Fiz. Elem. Chastits At. Yadra 8, 429 (1977) [Sov. J. Part. Nucl. 8, 175 (1977)].
[40]M. I. Strikman and L. L. Frankfurt, Fiz. Elem. Chastits At. Yadra 11, 571 (1980) [Sov. J. Part. Nucl. 11, 221 (1980)].
[41]V. I. Komarov, in: Materialy XIV zimneĭ shkoly LIYaF (Proc. of the 14th Winter School of the Leningrad Institute of Nuclear Physics), LINP (1979), pp. 71–113.
[42]Yu. P. Yakovlev, Fiz. Elem. Chastits At. Yadra 8, 255 (1977) [Sov. J. Part. Nucl. 8, 106 (1977)].
[43]V. S. Barashenkov and V. D. Toneev, Vzaimodeĭstviya vysokoénergeticheskikh chastits i atomnykh yader s yadrami (Interactions of High-Energy Particles and Nuclei with Nuclei), Atomizdat, Moscow (1972).
[44]K. K. Gusima, S. G. Mashnik, and V. D. Toneev, in: Raschety struktury yadra i yadernykh reaktsiĭ (Calculations of Nuclear Structure and Nuclear Reactions), Shtiintsa, Kishinev (1977), pp. 12–18.
[45]K. K. Gudima, S. G. Mashnik, and V. D. Toneev, Soobshchenie (Communication) R2-80-777, JINR, Dubna (1980).
[46]Yu. P. Yakovlev, Yad. Fiz. 30, 1240 (1979) [Sov. J. Nucl. Phys. 30, 646 (1979)].
[47]V. E. Bunakov, Izv. Akad. Nauk SSSR, Ser. Fiz. 45, 140 (1981).
[48]O. V. Lozhkin and Yu. P. Yakovlev, Izv. Akad. Nauk SSSR, Ser. Fiz. 21, 315 (1967).
[49]E. L. Grigor'ev, O. V. Lozhkin, V. M. Mal'tsev, and Yu. P. Yakovlev, Yad. Fiz. 6, 696 (1967) [Sov. J. Nucl. Phys. 6, 507 (1967)].
[50]A. A. Nosov, V. V. Smirnov, A. A. Rimskiĭ-Korsakov, and Yu. P. Yakovlev, Preprint RI-87 [in Russian], V. G. Khlopin Radium Institute, Leningrad (1978).
[51]G. M. Raisbeck and F. Yiou, Phys. Rev. C 12, 915 (1975).
[52]N. T. Porile, G. D. Cole, and C. R. Rudy, Phys. Rev. C 19, 2288 (1979).
[53]V. M. Zaĭtsev, G. D. Alkhazov, and V. K. Veselov, Preprint No. 414 [in Russian], Physicotechnical Institute, Leningrad (1972).
[54]J. Stewenson, P. B. Price, and K. Frankel, Phys. Rev. Lett. 38, 1125 (1977).
[55]J. P. Alard, A. Baldit, R. Brun, *et al.*, Nuovo Cimento A30, 320 (1975).
[56]G. M. Raisbeck, P. Boerstling, R. Klapisch, and T. D. Thomas, Phys. Rev. C 12, 527 (1975).
[57]R. E. L. Green and R. G. Korteling, Phys. Rev. C 18, 311 (1978).
[58]R. E. L. Green and R. G. Korteling, Phys. Rev. C 22, 1594 (1980).
[59]H. D. O'Brien, P. M. Grant, and A. E. Ogard, "The LASL medical radioisotope research program: radiochemistry problems and new developments," in: Progress in Nuclear Medicine, Vol. 4, Medical Cyclotrons in Nuclear Medicine, S. Karger, New York (1978).
[60]J. R. Wu, C. C. Chang, and H. D. Holmgren, Phys. Rev. C 19, 659 (1979).
[61]J. R. Wu, C. C. Chang, and H. D. Holmgren, Phys. Rev. C 19, 698 (1979).
[62]S. B. Kaufman, M. W. Weisfield, E. P. Steinberg, *et al.*, Phys. Rev. C 19, 962 (1979).
[63]H. H. Heckman, D. E. Greiner, P. J. Lindstrom, and F. S. Biser, Preprint LBL-596, Berkeley (1972).
[64]V. A. Plyushchev and Yu. P. Yakovlev, Preprint RI-142 [in Russian], V. G. Khlopin Radium Institute, Leningrad (1981).
[65]S. A. Khorozov, Soobshchenie (Communication) I-12276, JINR, Dubna (1979).
[66]K. Le Couter, in: Yadernye reaktsii (Nuclear Reactions), Vol. 2, Gosatomizdat, Moscow (1962), pp. 309–344.
[67]V. I. Bogatin, E. A. Ganza, O. V. Lozhkin, *et al.*, Yad. Fiz. 34, 104 (1981) [Sov. J. Nucl. Phys. 34, 59 (1981)].
[68]A. A. Arakelyan, G. V. Arustamyan, A. S. Danagulyan, *et al.*, Yad. Fiz. 35, 518 (1982) [Sov. J. Nucl. Phys. 35, 298 (1982)].
[69]V. K. Lukyanov and A. I. Titov, Phys. Lett. 57B, 10 (1975).
[70]N. Masuda, I. Katsumi, and I. Yoshihito, Phys. Lett. 23C, 1543 (1981).
[71]V. I. Bogatin, E. A. Ganza, O. V. Lozhkin, *et al.*, Yad. Fiz. 31, 845 (1980) [Sov. J. Nucl. Phys. 31, 436 (1980)].
[72]V. I. Bogatin, E. A. Ganza, O. V. Lozhkin, *et al.*, Preprint RI-139 [in Russian], V. G. Khlopin Radium Institute, Leningrad (1981).
[73]V. I. Bogatin, E. A. Ganza, O. V. Lozhkin, *et al.*, Yad. Fiz. 36, 33 (1982) [Sov. J. Nucl. Phys. 36, 19 (1982)].
[74]A. M. Zebelman, A. M. Poskanzer, J. D. Bowman, *et al.*, Phys. Rev. C 11, 1280 (1975).
[75]Yu. P. Yakovlev, Yad. Fiz. 32, 415 (1980) [Sov. J. Nucl. Phys. 32, 214 (1980)].
[76]K. K. Gudima, S. G. Mashnik, and V. D. Toneev, Soobshchenie (Communication) E2-11307, JINR, Dubna (1978).
[77]N. A. Perfilov, O. V. Lozhkin, and V. I. Ostroumov, Yadernye reaktsii pod deĭstviem chastits vysokikh énergiĭ (Nuclear Reactions Induced by High-Energy Particles), USSR Academy of Sciences, Leningrad (1962).
[78]S. M. Eliseev, Soobshchenie (Communication) R2-4160, JINR, Dubna (1968).
[79]E. K. Hyde, G. W. Butler, and A. M. Poskanzer, Phys. Rev. C 4, 1759 (1971).
[80]A. M. Poskanzer, G. W. Butler, and E. K. Hyde, Phys. Rev. C 3, 882 (1971).
[81]E. N. Vol'nin, A. A. Borob'ev, V. G. Grachev, *et al.*, Preprint No. 101 [in Russian], Leningrad Institute of Nuclear Physics, Leningrad (1974).
[82]V. V. Aldeichikov, Phys. Lett. 92B, 74 (1980).
[83]V. S. Stavinskiĭ, Fiz. Elem. Chastits At. Yadra 3, 832 (1972) [Sov. J. Part. Nucl. 3, 417 (1972)].
[84]K. Seidel, D. Seeliger, R. Reif, and V. D. Toneev, Fiz. Elem. Chastits At. Yadra 7, 499 (1976) [Sov. J. Part. Nucl. 7, 192 (1976)].
[85]O. V. Lozhkin, V. S. Oplavin, and Yu. P. Yakovlev, Preprint RI-156 [in Russian], V. G. Khlopin Radium Institute, Leningrad (1982).
[86]V. S. Barashenkov, Z. M. Zadorozhnyĭ, and B. F. Kostenko, Preprint R2-12503 [in Russian], JINR, Dubna (1979).
[87]V. D. Toneev, Problems of the Interaction of particles and the lightest nuclei with nuclei in the region of intermediate and high energies" [in Russian] (Author's Abstract of

Doctoral Dissertation), JINR, Dubna (1979).
[88]H. W. Bertini, A. H. Culkowski, O. W. Hermann, *et al.*, Phys. Rev. C **17**, 1382 (1978).
[89]Y. Yariv and Z. Fraenkel, Phys. Rev. C **20**, 2227 (1979).
[90]W. D. Meyers and W. J. Swiatecki, Preprint UCRL-11980, Berkeley (1965).
[91]C. W. Jager, H. de Vries, and C. de Vries, At. Data Nucl. Data Tables **14**, 479 (1974).
[92]F. Ajzenberg-Selove, Nucl. Phys. **A227**, 1 (1974).
[93]F. Ajzenberg Selove, Nucl. Phys. **A281**, 1 (1977).
[94]F. Ajzenberg Selove, Nucl. Phys. **A248**, 1 (1975).
[95]M. P. Ivanova, V. S. Kurbatov, and V. M. Sidorov, Soobshchenie (Communication) 1-119P, JINR, Dubna (1978).
[96]F. C. Williams, Phys. Lett. **31B**, 184 (1970).
[97]V. V. Avdeĭchikov, E. L. Grigor'ev, O. V. Lozhkin, and Yu. P. Yakovlev, Soobshchenie (Communication) R-2093, JINR, Dubna (1965).
[98]V. I. Bogatin, O. V. Lozhkin, and Yu. P. Yakovlev, Preprint RI-45 [in Russian], V. G. Khlopin Radium Institute, Leningrad (1976).
[99]V. S. Vasilevskiĭ, T. P. Kovalenko, and G. F. Filippov, in: Tezisy dokladov XXXI soveshchaniya po yadernoĭ spektroskopii i strukture atomnogo yadra (Abstracts of Papers at the 31st Symposium on Nuclear Spectroscopy and Nuclear Structure), Samarkand, April 14–16, 1981, Nauka, Leningrad (1980).
[100]A. H. Wapstra, Ark. Fys. **36**, 329 (1967).
[101]V. Ya. Antonchenko and I. V. Simenog, Preprint ITF-78-103R [in Russian], Institute of Theoretical Physics, Kiev (1978).
[102]N. T. Porile, B. J. Dropesky, and B. A. Williams, Phys. Rev. C **18**, 2231 (1978).
[103]Y. Y. Chu, G. Friedlander, and L. Husain, Phys. Rev. C **15**, 352 (1977).
[104]H. Raun, J. Inorg. Nucl. Chem. **31**, 1883 (1969).
[105]E. Hageb, J. Inorg. Nucl. Chem. **29**, 2515 (1967).
[106]J. Chaumont, Thesis [in French], Faculté des Sciences d'Orsay, University of Paris (1970).
[107]B. N. Belyaev *et al.*, Nucl. Phys. **A348**, 479 (1980).
[108]V. D. Domkin, "Experimental investigation of isotopic effects in disintegration reactions and fission induced by 1-GeV protons" [in Russian], Author's Abstract of Candidate's Dissertation, V. G. Khlopin Radium Institute, Leningrad (1982).
[109]L. Kh. Batist, S. D. Golos, V. S. Gusel'nikov, and Yu. P. Yakovlev, Preprint No. 677 [in Russian], Leningrad Institute of Nuclear Physics, Leningrad (1981).
[110]G. M. Raisbeck, J. Lestrinquez, and F. Yiou, Nat. Phys. Sci. **244**, 28 (1973).
[111]M. Ephere and E. Gradstajn, J. Phys. (Paris) **28**, 745 (1967).
[112]M. Barbier and S. Regnier, J. Inorg. Nucl. Chem. **33**, 2720 (1968).
[113]J. Dostrovsky, H. Gauvin, and M. Lefort, Phys. Rev. **169**, 836 (1968).
[114]G. V. S. Rayundu, Can. J. Chem. **42**, 1149 (1964).
[115]J. R. Radin, E. Gradstajn, and A. R. Smith, Phys. Rev. C **20**, 787 (1979).
[116]W. Loveland, L. Cheng, P. L. McGoughney, *et al.*, Phys. Rev. C **24**, 464 (1981).
[117]S. B. Kaufman, M. W. Weisfield, B. D. Wilkins, and D. J. Henderson, Phys. Rev. C **22**, 1897 (1980).
[118]S. B. Kaufman and M. W. Weisfield, Phys. Rev. C **11**, 1258 (1975).
[119]H. Sauvageon, S. Regnier, and G. N. Simonoff, Phys. Rev. C **25**, 466 (1982).
[120]J. A. Urbon, S. B. Kaufman, D. J. Henderson, and E. P. Steinberg, Phys. Rev. C **21**, 1048 (1980).
[121]D. R. Fortney and N. T. Porile, Phys. Rev. C **21**, 664 (1980).
[122]V. N. Arutyunyan, G. V. Badalyan, D. M. Beglaryan, *et al.*, Vopr. At. Nauki Tekh., Ser. Obshch. Yad. Fiz. No. 4, 3 (1981).
[123]A. V. Efremov, Fiz. Elem. Chastits At. Yadra **13**, 613 (1982) [Sov. J. Part. Nucl. **13**, 254 (1982)].
[124]M. Lemaire, C. Nagamia, S. Schnetzer, *et al.*, Phys. Lett. **85B**, 38 (1979).
[125]D. I. Blokhintsev, Zh. Eksp. Teor. Fiz. **33**, 1295 (1957) [Sov. Phys. JETP **6**, 995 (1958)].
[126]O. V. Lozhkin, N. A. Perfilov, and Yu. P. Yakovlev, Preprint R-1734 [in Russian], JINR, Dubna (1964).
[127]O. V. Lozhkin and Yu. P. Yakovlev, in: Programma i tezisy dokladov XIV ezhegodnogo soveshchaniya po yadernoĭ spektroskopii v Tbilisi 14–22 Fevralya 1964 g. (Program and Abstracts of Papers at the 14th Annual Symposium on Nuclear Spectroscopy at Tbilisi, February 14–22, 1964), Nauka, Leningrad (1963), p. 110.
[128]E. L. Grigor'ev and O. V. Lozhkin, Preprint 1-5245 [in Russian], JINR, Dubna (1970).
[129]D. H. Boal, R. E. L. Green, R. G. Korteling, and M. Soroushian, Phys. Rev. C **23**, 2788 (1981).
[130]J. Kapusta, Phys. Rev. C **24**, 2545 (1981).
[131]J. Gosset, J. I. Kapusta, and G. D. Westfall, Phys. Rev. C **18**, 844 (1978).
[132]L. Kh. Batist, E. N. Vol'nin, V. P. Grachev, *et al.*, Preprint No. 606 [in Russian], Leningrad Institute of Nuclear Physics, Leningrad (1980).
[133]Yu. A. Murin, "Production of helium and lithium isotopes with large transverse momenta in collisions of 6.6-GeV protons with nuclei" [in Russian], Author's Abstract of Candidate's Dissertation, V. Kh. Khlopin Radium Institute, Leningrad (1981).
[134]M. M. Nesterov, V. F. Petrov, and N. A. Tarasov, Yad. Fiz. **35**, 1131 (1982) [Sov. J. Nucl. Phys. **35**, 662 (1982)].
[135]A. Z. Mekjian, Nucl. Phys. **A384**, 492 (1982).

Translated by Julian B. Barbour